Biomimatic material(생체 모방 재료)의 조직 공학에 대한 연구동향

Chung-Ang University, Da Vinci College of General Education
OK JA Yoon

CHERIC
Chemical Engineering and Materials Research Information Center
국가지정
화학공학소재연구정보센터

연구 동향

✓ **Development of an Anti-Inflammatory Drug-Incorporated Biomimetic Scaffold for Corneal Tissue Engineering[1]**

- 이 연구의 목표는 naproxen sodium (NS)이 포함된 다공성 poly(lactide-co-glycolide) 지지체 (NS-incorporated PLGA scaffold)를 생체 모방하여 디자인함으로써 효과적인 각막 손상 치료에 응용하고자 개발함.

- NS-incorporated PLGA 지지체는 동결건조에 의해 만들었으며 세포 부착성이 좋은 collagen이나 poly-l-lysin으로 표면을 코팅하였음. 동결 건조된 지지체는 50~200μm 크기의 다공성을 가지고 있음을 확인하였고 세포의 구멍 구조 (open-cellular pore structures)와 비슷한 구조를 형성함.

- 또한 약물 저장 효율이 84% 보다 높았으며 약 90~98%의 NS가 7일 동안 유지하였으며 초기에 빠르게 약물이 방출하였고 그 이후에 천천히 지속적으로 약물을 방출함을 확인함.

- 뉴질랜드의 흰 토끼에서 분리한 각막상피 세포를 이 지지체 위에 배양했을 때, 적어도 10일 동안 독성 효과 없이 증식함을 확인함으로써 NS-incorporated PLGA 지지체는 약물 방출을 조절하면서 각막 손상 치료뿐만 아니라 생물 의학적 적용 가능성을 확인함.

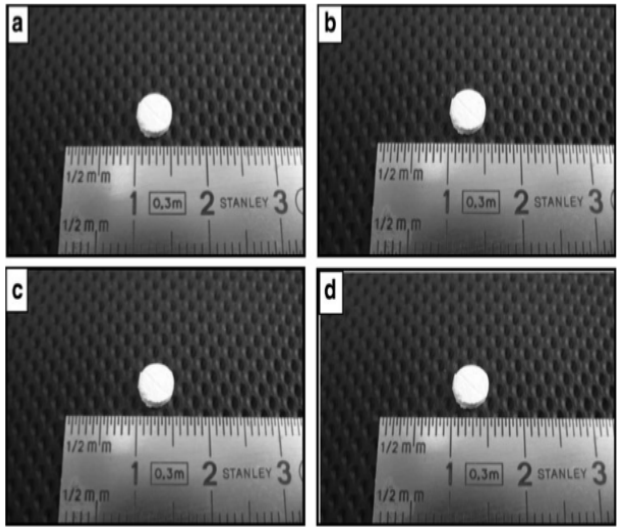

FIG. 1. Photograph of blank or NS-loaded PLGA scaffolds; **(a)** PLGA50-B, **(b)** PLGA50-NS, **(c)** PLGA75-B, and **(d)** PLGA75-NS. NS, naproxen sodium; PLGA, poly(lactide-*co*-glycolide).

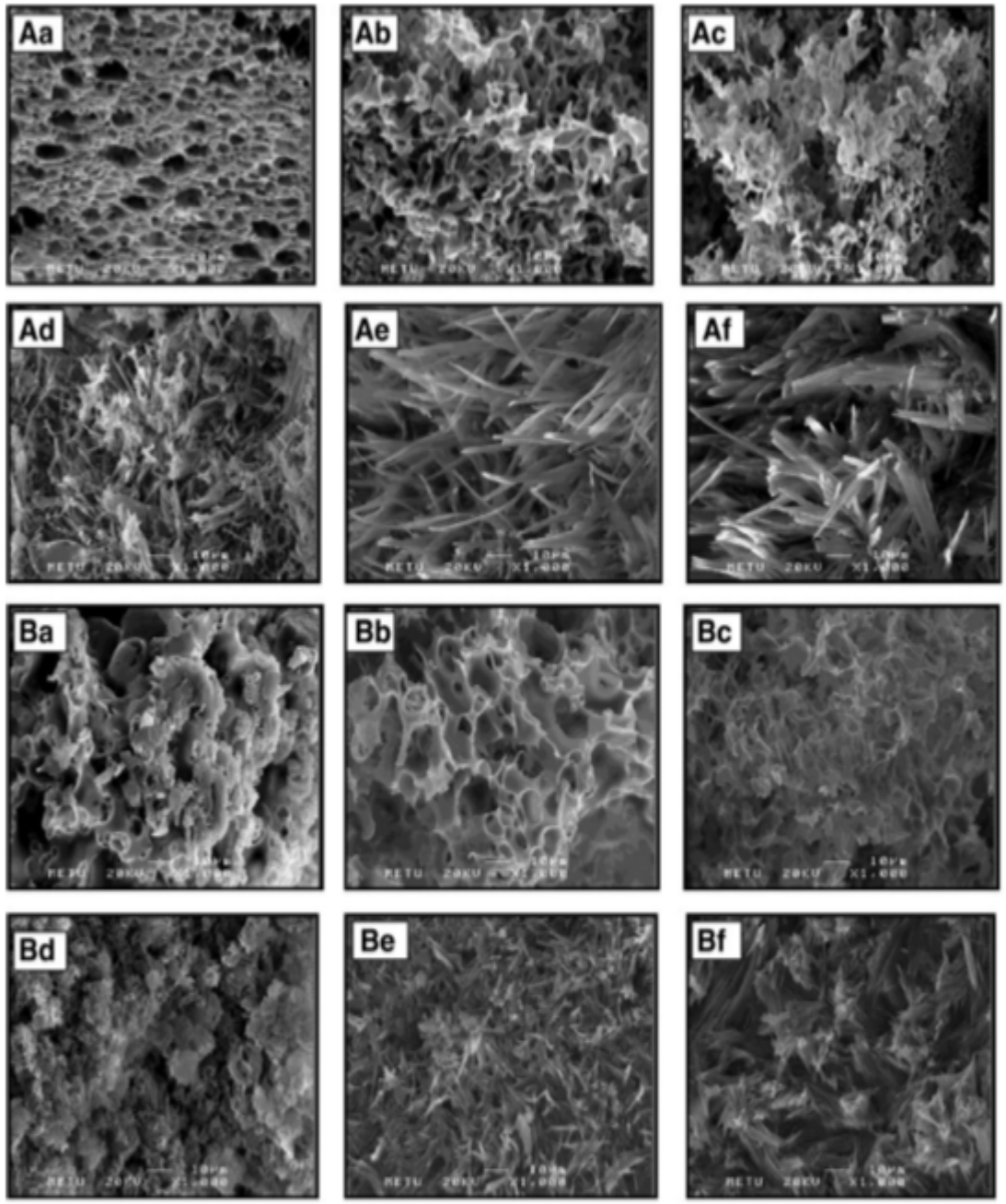

FIG. 2. Cross-sectional SEM images of blank or NS-loaded PLGA scaffolds; **(Aa)** PLGA50-B, **(Ab)** PLGA50-B-K, **(Ac)** PLGA50-B-L; **(Ad)** PLGA50-NS, **(Ae)** PLGA50-NS-K, **(Af)** PLGA50-NS-L; **(Ba)** PLGA75-B, **(Bb)** PLGA75-B-K, **(Bc)** PLGA75-B-L; **(Bd)** PLGA75-NS, **(Be)** PLGA75-NS-K, and **(Bf)** PLGA75-NS-L. SEM, scanning electron microscope.

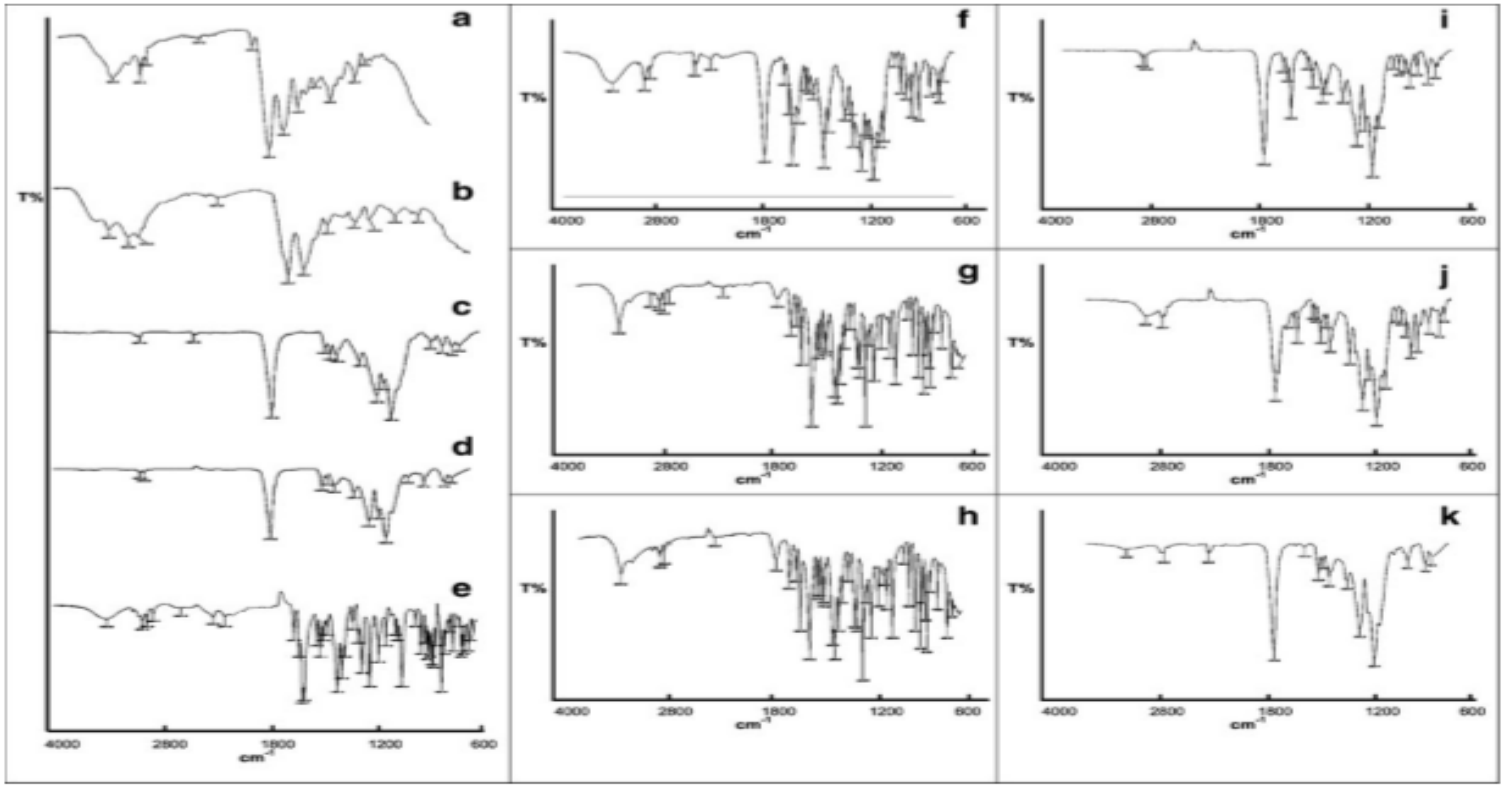

FIG. 3. FTIR absorption spectra of **(a)** collagen, **(b)** poly-L-lysine, **(c)** PLGA50-B, **(d)** PLGA75-B, **(e)** NS, **(f)** PLGA50-NS, **(g)** PLGA50-NS-K, **(h)** PLGA50-NS-L, **(i)** PLGA75-NS, **(j)** PLGA75-NS-K, and **(k)** PLGA75-NS-L. FTIR, Fourier transform infrared.

TABLE 1. FORMULATION CODES, PORE DIAMETERS, AND TENSILE STRENGTHS OF POLY(LACTIDE-*CO*-GLYCOLIDE) SCAFFOLDS

Formulation	*Code*	*Pore diameter (μm)*[a]	*Tensile strength (N/m^2) ($\times 10^6$)*
Blank (without drug) scaffolds			
PLGA (50:50)	PLGA50-B	173.3 ± 17.3	0.246 ± 0.001
PLGA (50:50) coated with collagen	PLGA50-B-K	168.7 ± 21.0	0.270 ± 0.012
PLGA (50:50) coated with poly-L-lysine	PLGA50-B-L	169.5 ± 20.6	0.219 ± 0.011
PLGA (75:25)	PLGA75-B	168.3 ± 20.4	0.553 ± 0.056
PLGA (75:25) coated with collagen	PLGA75-B-K	168.7 ± 20.9	0.476 ± 0.026
PLGA (75:25) coated with poly-L-lysine	PLGA75-B-L	169.4 ± 20.5	0.457 ± 0.047
NS-incorporated scaffolds			
PLGA (50:50)—NS	PLGA50-NS	164.2 ± 11.9	0.343 ± 0.077
PLGA (50:50) coated with collagen—NS	PLGA50-NS-K	163.8 ± 11.8	0.156 ± 0.016
PLGA (50:50) coated with poly-L-lysine—NS	PLGA50-NS-L	164.1 ± 12.0	0.222 ± 0.038
PLGA (75:25)—NS	PLGA75-NS	163.9 ± 11.7	0.312 ± 0.252
PLGA (75:25) coated with collagen—NS	PLGA75-NS-K	163.3 ± 11.7	0.155 ± 0.037
PLGA (75:25) coated with poly-L-lysine—NS	PLGA75-NS-L	163.8 ± 11.9	0.134 ± 0.040

[a]Mean ± standard deviation ($n = 3$).
NS, naproxen sodium; PLGA, poly(lactide-*co*-glycolide).

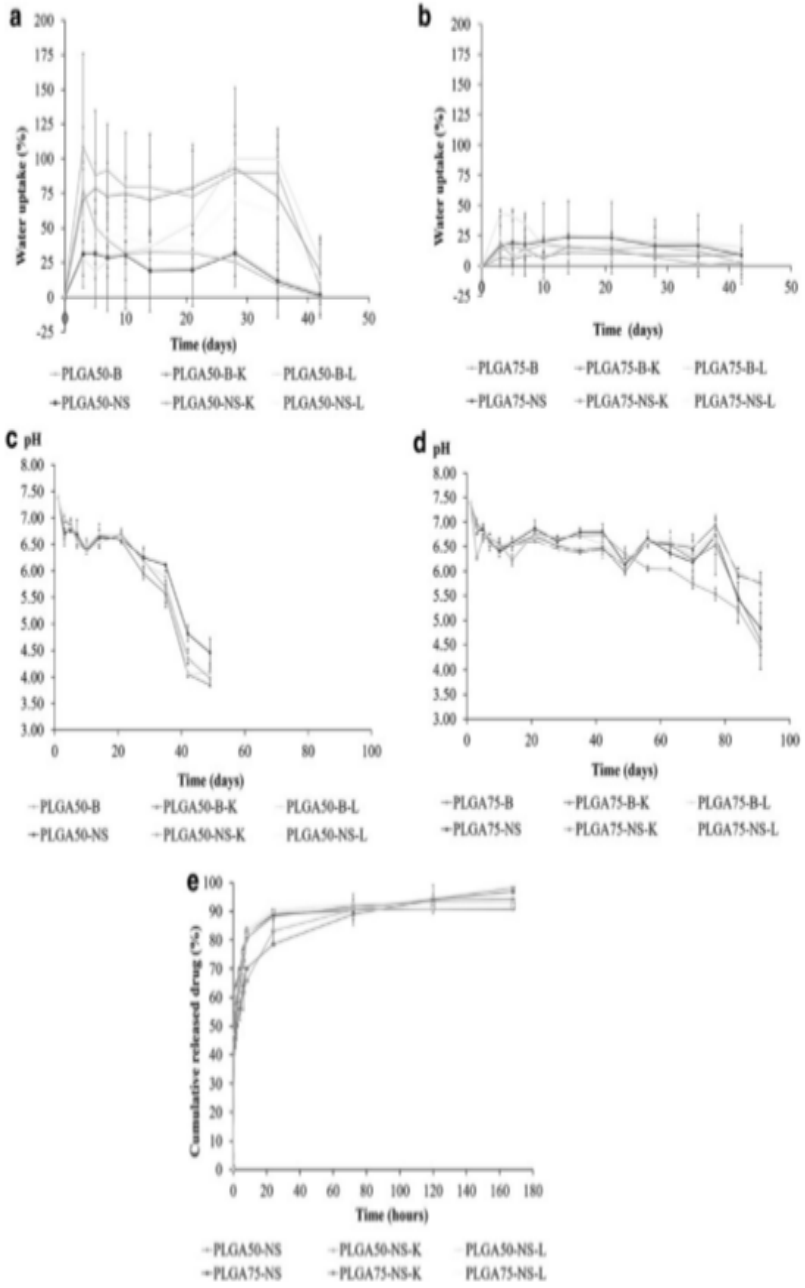

FIG. 4. Water uptake (**a, b**), degradation test (**c, d**), and cumulative drug release study (**e**) results of PLGA 50 or PLGA 75 scaffolds ($n = 6$).

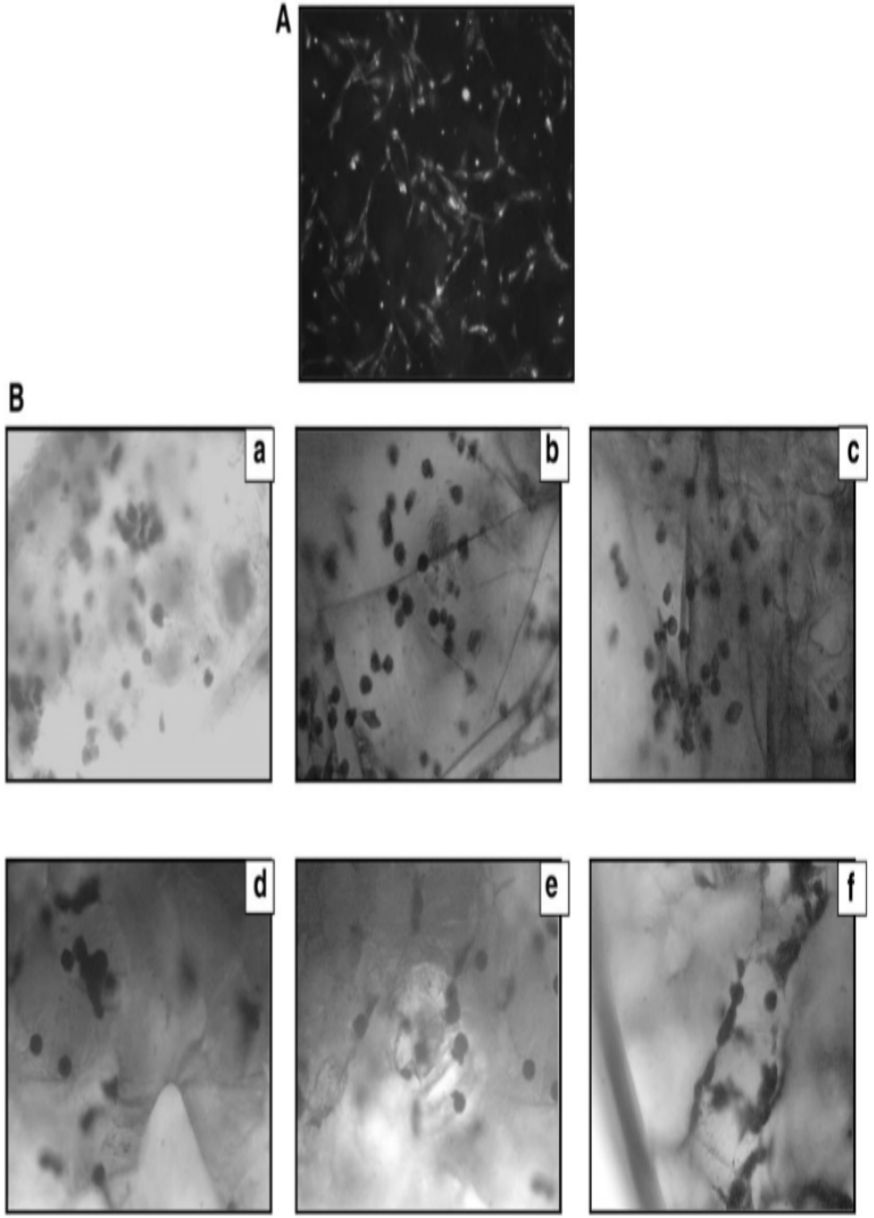

FIG. 5. (**A**) Fluorescence microscope photographs of corneal epithelial cells stained with cytokeratin 14. (**B**) Optical microscope photographs of NS-loaded PLGA scaffolds stained with Giemsa; (**a**) PLGA50-NS, (**b**) PLGA50-NS-K, (**c**) PLGA50-NS-L, (**d**) PLGA75-NS, (**e**) PLGA75-NS-K, and (**f**) PLGA75-NS-L.

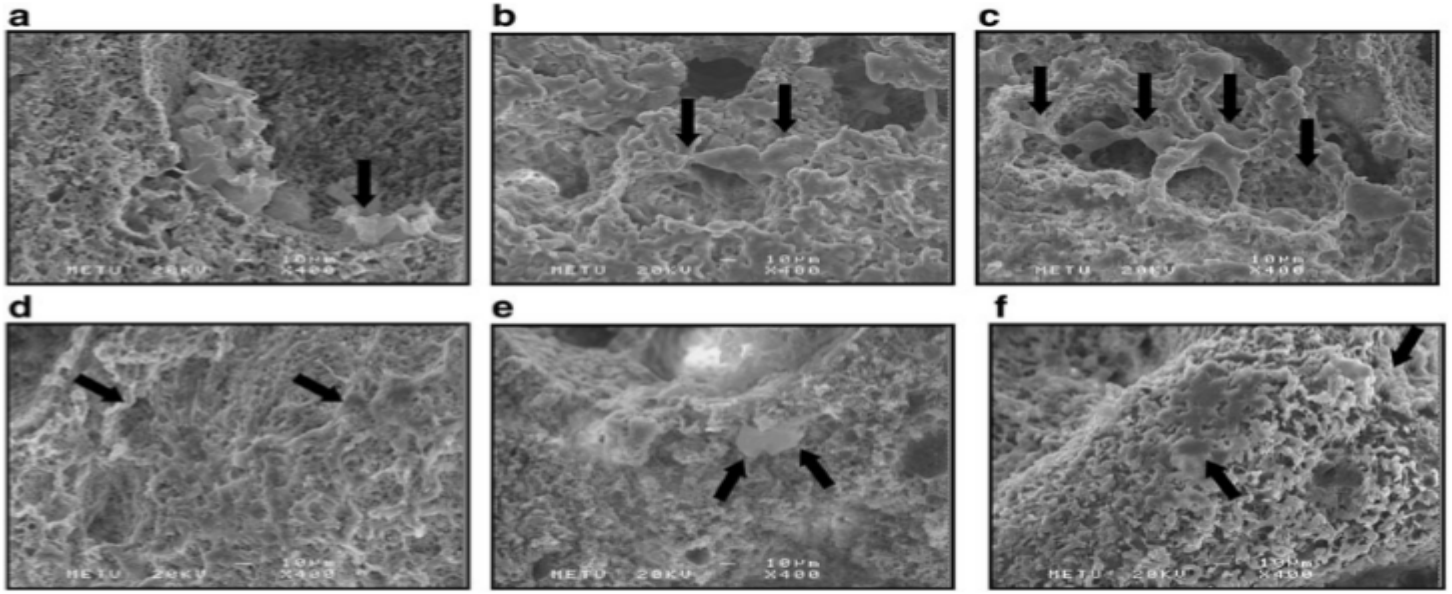

FIG. 6. SEM photographs of corneal epithelial cells grown in the interiors of NS-loaded PLGA scaffolds at 3 days after culture (*arrow* indicates cells attached); **(a)** PLGA50-NS, **(b)** PLGA50-NS-K, **(c)** PLGA50-NS-L, **(d)** PLGA75-NS, **(e)** PLGA75-NS-K, and **(f)** PLGA75-NS-L.

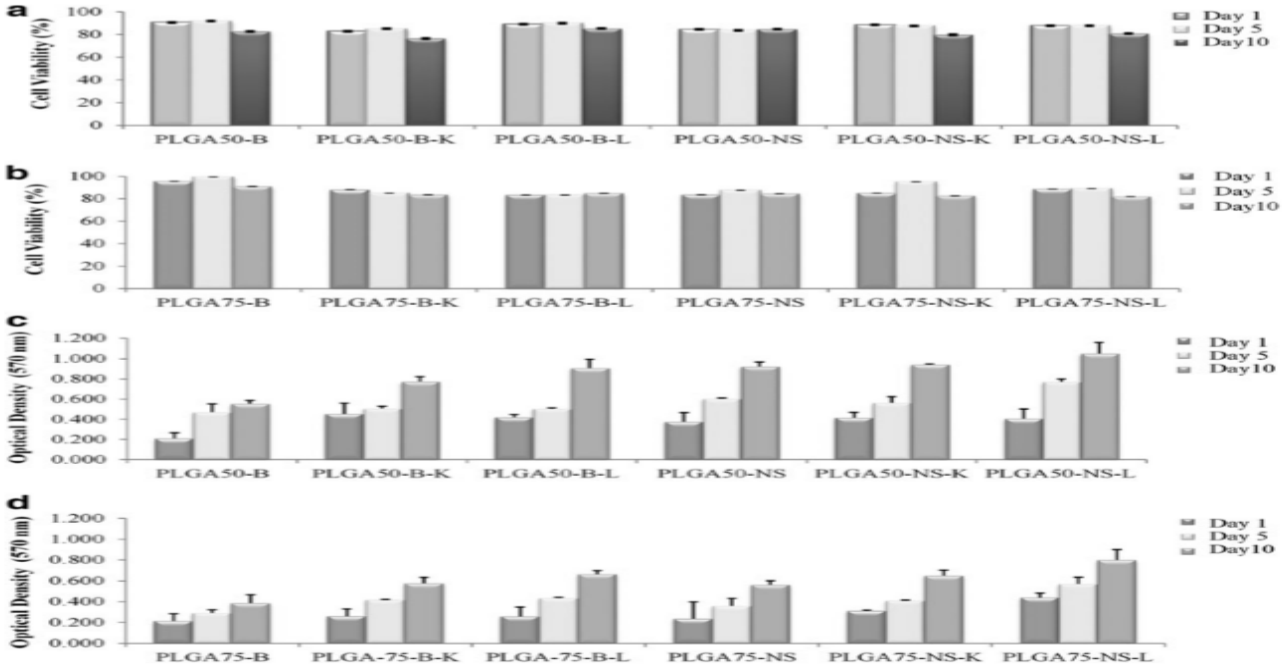

FIG. 7. Cytotoxicity of PLGA scaffolds against the corneal epithelial cells ($n = 6$) **(a, b)**. Proliferation profiles of corneal epithelial cells grown on PLGA scaffolds ($n = 6$) **(c, d)**.

✓ 3D printing of biomimetic vasculature for tissue regeneration[2]

- 조직 공학에 있어서 중요한 임상 적용의 한계점은 장기간 동안 대량 수송 능력 (long-range mass transport capability)의 부족으로 인한 복잡한 3D 조직 (complex three dimensional (3D) tissues) 개발이 어렵다는 문제를 가지고 있음.

- 단일 포트 3D 프린터 (One-pot 3D printer)로 만든 카레멜 기반 템플릿(sacrificial caramel templates)을 만들어 폴리머 용액에 담군 다음 유기용매가 휘발되면서 위상분리 (integrated phase separation)를 통해 폴리머로 코팅한 후 카라멜 템플릿을 제거함으로써 perfusable and permeable hierarchical micro channel networks (PHMs)를 개발함.

- 패턴화된 PHMs는 제어 가능한 마이크로 공극을 가진 투과성 벽과 상호 연결된 마이크로채널 (micro-channels), 맞춤형 확장 가능한 3D 프레임워크를 포함한 생체 모방형 3D 혈관 구조를 가지고 있으며, 이러한 제작 과정은 박테리아 셀룰로오즈, 전기방사된 나노섬유, 입자를 걸러낼 수 있는 다공성 지지체, 하이드로 겔을 포함한 다양한 메트릭스와 폴리머를 가지고 개발 가능성을 제시함.

- 이러한 개발은 체외 (in vitro)에서 PHMs가 심장 세포의 대사 기능을 유지하고, 체내 (in vivo)에서 혈관신생 (angiogenesis)과 조직 공학, 심근경색 (myocardial infarction)에 효율적으로 치료할 수 있다는 것을 입증함으로써 조직 공학 구조에서 PHMs의 다양성을 입증함.

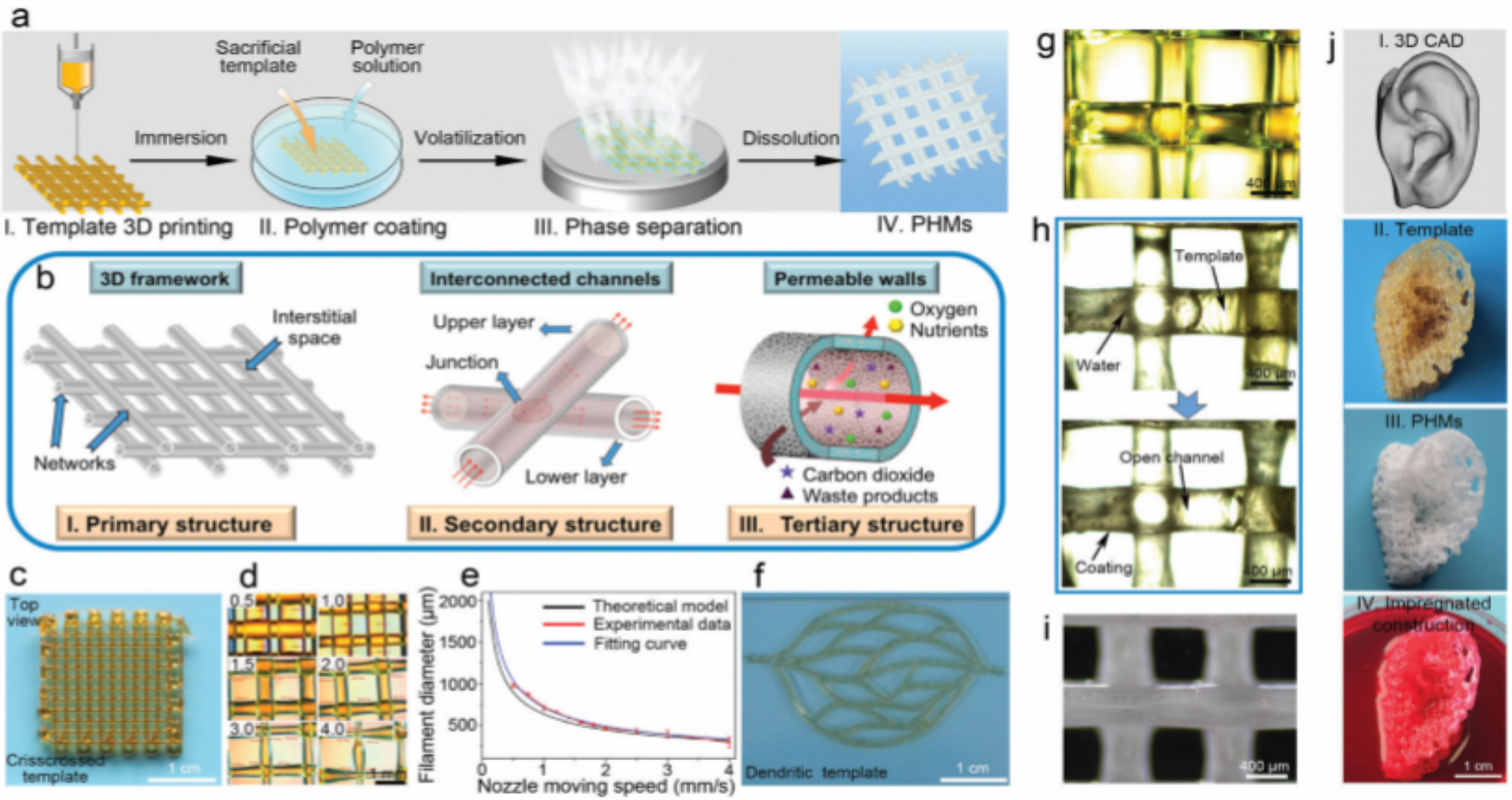

Fig. 1 Design and fabrication of PHMs. (a) Schematic illustration of the fabrication process. (I) 3D printing of the caramel-based template using fused deposition modeling. (II) Thin polymer coating on the template *via* solution casting. (III) Modulation of the microstructure of the polymer coating based on phase separation during solvent volatilization. (IV) PHM formation upon removal of the template. (b) Schematic diagrams of the PHMs with hierarchical architectures. (I) Primary structure: multilayered network on the macro scale provided tailorable and scalable scaffolds. (II) Secondary structure: interconnected polymeric channels with smooth junctions facilitated the mass transportation in the whole scaffold. (III) Tertiary structure: porous channel walls enabled mass exchange inside and outside of the channels. (c) Top view of the crisscross caramel-based template. (d) Optical images of templates with different filament diameters. (e) The filament diameters were well controlled by the nozzle travel speed in an exponential relationship. (f) A sophisticated template with multi-branched and curving filaments could be 3D-printed. (g) Top view of the magnified 3D caramel-based template. (h) Distilled water added from one side of the polymer (PCL) coated template could quickly dissolve the caramel filaments and went through the whole template leading to interconnected polymer channels in minutes. (i) The optical microscope images of the resultant PHMs. (j) CAD/CAM process for tailoring PHMs imitating a specific tissue or organ exemplified by a human ear. A 3D CAD model offered the visualized motion path to precisely control the macro-framework and micro-structure of the caramel-based template. The reverse molding fabricated PCL PHMs in an ear-shape framework constructed by an interconnected hollow channel network with efficient long-term mass transportation ability demonstrated by the perfusion of red dye.

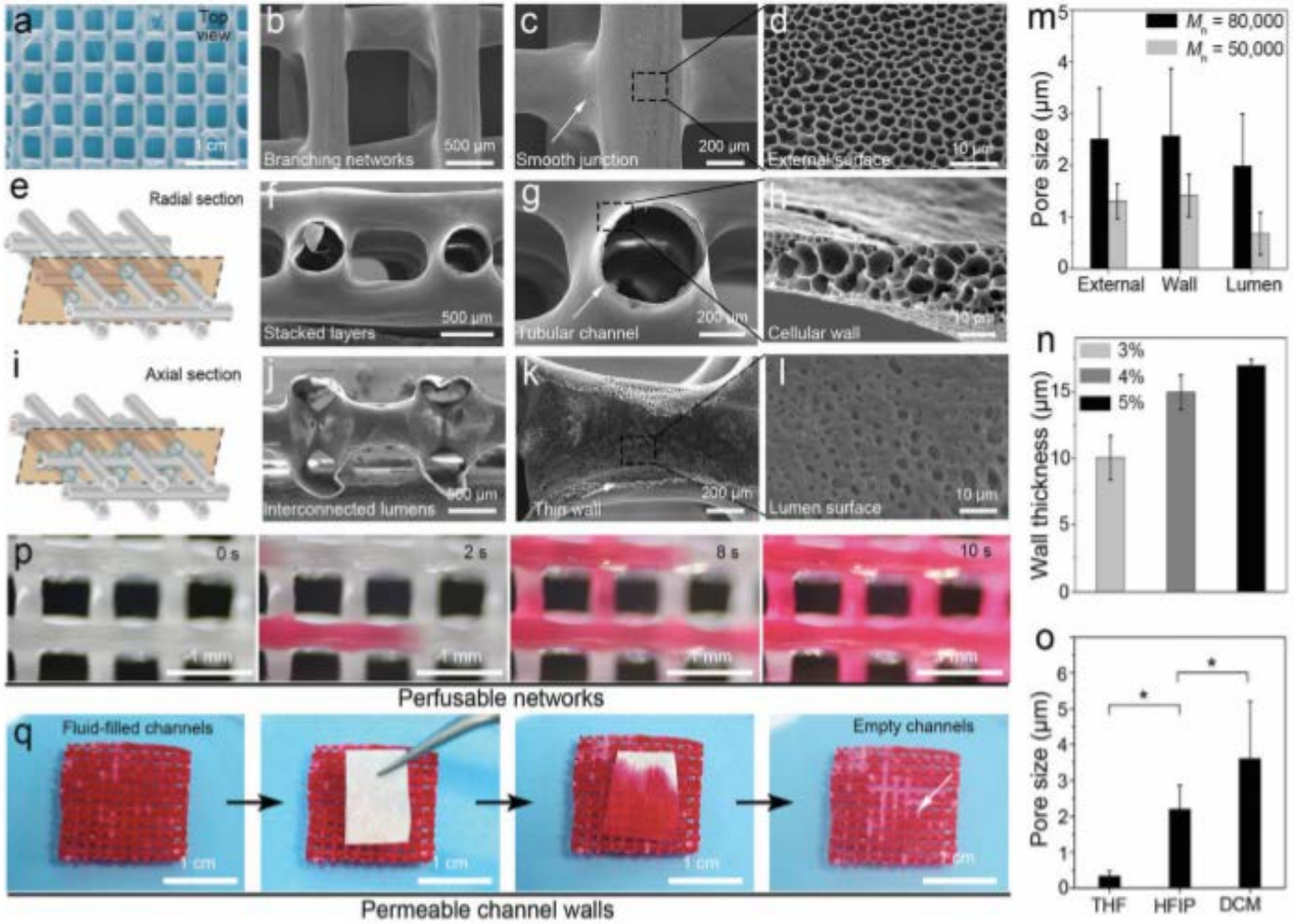

Fig. 2 Morphology and mass exchange ability of PCL PHMs. Optical image (a) and SEMs (b–d) of HMW-PCL PHMs in top view. Diagram (e) and SEMs (f–h) of the side view in the radial direction. Diagram (i) and SEMs (j–l) of the side view in the axial direction. PHMs showed hierarchical structures including multiple layered networks (b, f and j; primary structure), interconnected hollow tubular channels with smooth junctions (c, g and k; secondary structure) and porous structures throughout the channels walls (d, h and l; tertiary structure; external surface, inside of wall and lumen surface). (m) The pores of PHMs from HMW-PCL were relatively larger than those from LMW-PCL. (n) PHMs made from higher concentrations exhibited thicker walls. (o) The pores of PHMs from HFIP solution casting were relatively larger than the pores of PHMs from THF and smaller than the pores of PHMs from DCM. (p) Time-lapse microscope images of the perfusion of red dye fluid through the branching channels of PHMs upon injection from one end. (q) Time-lapse images of absorbing red dye fluid of outside blotting paper from lumens of PHMs through the porous channel walls.

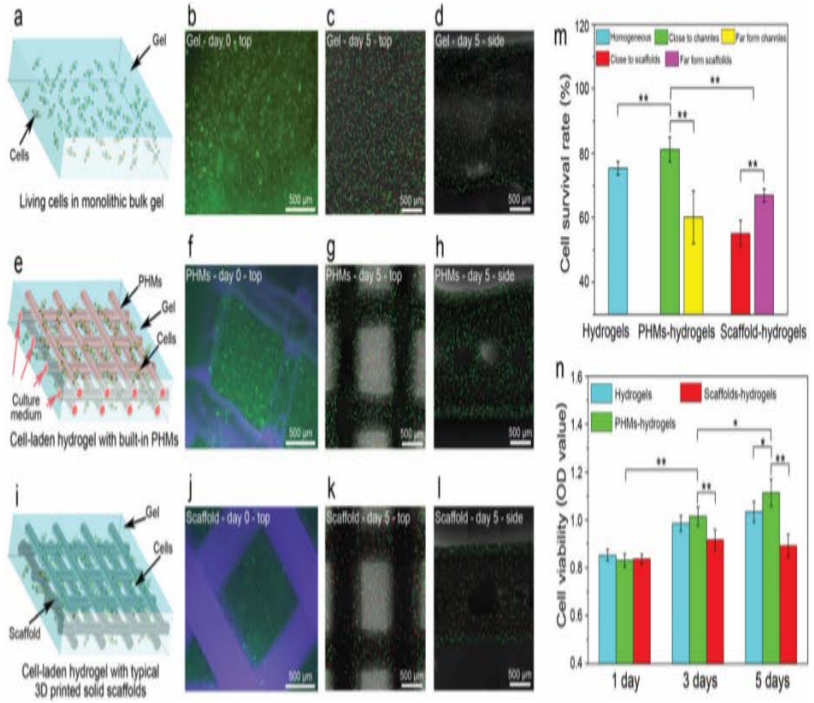

Fig. 3 PHMs sustained cellular metabolic function at high cell densities. (a–l) Engineered cardiac tissue constructs. PCL PHMs were encapsulated in alginate hydrogels along with living rat cardiomyocytes (e–h, PHMs-hydrogels), compared with monolithic cell-laden alginate hydrogels (a–d) and typical 3D-printed solid PCL scaffold within cell-laden gels (i–l, scaffold-hydrogels). Representative fluorescence microscopic images (b, f and j) of live–dead staining right after cell seeding visualized the uniform distribution of cells in all three types of scaffolds. After 5 days culture, confocal micrographs of live–dead staining in monolithic bulk gel (c and d), PHM-hydrogels (g and h) and scaffold-hydrogels (k and l) in top view and representative cross-sectional views. Final images were stitched from multiple images of a confocal z-stack montage. (m) Cell survival rate in different groups and areas on days 5 (average ± s.d., $n = 4$). (n) CCK-8 assay demonstrated PHMs promoted cell viability and proliferation (average ± s.d., $n = 6$). *Statistically significance, *$p < 0.05$, **$p < 0.01$.

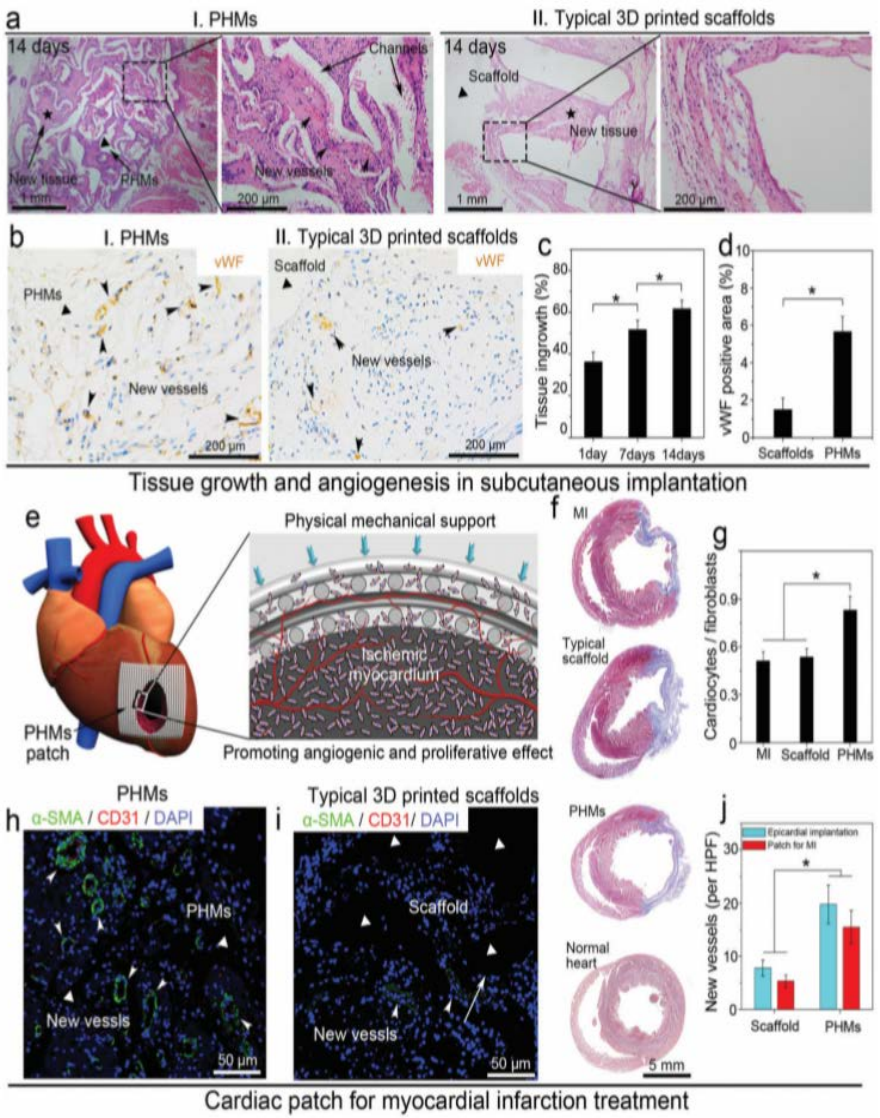

Fig. 4 PHMs facilitated angiogenesis and tissue integration in subcutaneous implantation and myocardial patch application. PHMs and typical 3D printed scaffolds (control group) in the same size (6 mm length × 6 mm width × 2 mm thickness) were implanted in subcutaneous (a–d) and myocardial regions (e–j) of Sprague Dawley rats. H&E staining (a) at predetermined time points (14 days post-implantation; $n = 3$). Immunohistochemical staining (b) of vWF for new vessels 14 days after implantation. Statistic quantification (c) of tissue integration rate of the PHMs group (average ± s.d., $n = 6$). Comparison of vessel regeneration rate (d) of PHMs and control groups (average ± s.d., $n = 6$) 14 days after implantation. Schematic diagram (e) of using PHMs as a myocardial patch. Masson staining (f) of ischemic heart, typical scaffold treated heart, PHMs patched heart and normal hearts at 4 weeks post-implantation (scale bar, 5 mm). The evaluation of fibrosis degree (g) in the myocardial area. Immunofluorescence staining of α-SMA (green), CD31 (red) and DAPI (blue) in the PHMs (h) and control group (i) for new vessels at 14 days post-implantation. The quantification of α-SMA and CD31 positive vessels (j). *Statistically significant, *$p < 0.05$.

✓ Mesenchymal stem cell 3D encapsulation technologies for biomimetic microenvironment in tissue regeneration[3]

- 중간엽 줄기 세포 (Mesenchymal stem cell, MSC) 캡슐화 기술은 손상된 조직을 복구하는데 있어 줄기 세포를 이식하는 중요한 역할로서 조직 공학 분야에서 오랫동안 개발되고 있음. MSC 캡슐화는 세포 생존력을 유지하고 MSC를 다중분화로 유도하는 3D 체내 환경의 모방을 입증함. 또한 MSC를 지지해주는 3D matrix는 사람의 선천적인 면역계로부터 MSC를 보호하고, 산소나 사이토카인 그리고 성장인자 같은 생분자가 확산할 수 있도록 도와주는 것을 보고함.

- 다양한 기술의 발달에 의해 MSC 캡슐화 플랫폼을 다양한 재료, 모양, 크기로 만들어낼 수 있게 되었으며 플랫폼의 조건은 표적화된 조직과 이식 방법에 따라 다름을 보고하고 있음.

- 이 리뷰는 micromolding, electrostatic droplet extrusion, microfluidics, bioprinting, 조직 공학적 응용과 같은 MSC 캡슐화 기술에 대하여 자세히 소개하고 있으며 마지막으로, 세포 치료 기반 조직 재생 방법으로서의 MSC 캡슐화 기술의 도전 및 향후 방향에 대해 논의하고 있음.

➢ MSC encapsulation technology

- 3D 세포 배양 시스템의 첫 시도는 1906년의 Ross Harrison에 의한 hanging drop tissue culture system이고 세포 캡슐화는 1964년 Chang에 의해 제안된 나일론 막을 이용하여 유화 방법에 의한 반투과성의 microcapsules로 처음 소개됨. 유화 방법 (emulsification methods), collagen-agarose, 펩타이드는 세포 배양을 위한 3D microenvironment으로 보고됨.

- Bead와 matrix 안에 세포 캡슐화 연구가 광범위하게 연구되었는데 그 중에 간단하면서도 안정적인 구조를 형성하는 방법으로 hydrogel bead 내에 cell을 감싸는 방법과 coaxial air jet application, the liquid jet method, macromolecular collagen type I matrix, injection and co-extrusion에 의해 만들어진 hollow fiber 그리고 UV에 의한 photopolymerization 등이 보고되고 있음.

- 최근 새롭게 발명되고 가장 널리 쓰이는 세포 캡슐화 기술은 micromolding, electrostatic droplet extrusion, microfluidics, bioprinting 등이 있는데 특히, microfluidics와 bioprinting이 가장 널리 쓰이고 있음.

- 또한 생체 재료나 세포가 외부 자극에 의해 반응하는 4D printing 기술이 개발되고 있으며 이러한 기술들이 세포 기반 치료 목적으로 MSC 캡슐화에 적용되고 있음.

- 표 1에 target tissues에 대한 다양한 재료와 MSC type의 캡슐화 기술을 정리하였음.

Table 1 Summary of encapsulation technologies with diverse materials and MSC types for different target tissues

Technologies		Benefits and limitations	Materials	MSC type	Target tissue	Reference
Micromolding		Benefits: - Controlled shape - Controlled size Limitations: - Batch process	Fibrin	Human bone marrow-derived stem cell	Blood vessel	[36]
			Alginate	Bone marrow-derived stem cell	Non-specific	[37]
			Polyethylene glycol (PEG)-based hydrogel	Human mesenchymal stem cells	Non-specific	[38]
Electrostatic droplet extrusion		Benefits: - Controlled droplet size - Uniform droplet size Limitations: - Materials constraints	Alginate	Rat adipose-derived stem cell	Non-specific	[50]
			Alginate	Human adipose-derived stem cell	Non-specific	[51]
			Alginate-lyase	Rat adipose-derived stem cell	Bone	[85]
Microfluidics	Droplet	Benefits: - Controlled monodispersity - Controlled dimensions and shape Limitations: - Non-scalable	Gelatin norbornene (GelNB) and PEG	Human bone marrow-derived stem cell	Hyaline cartilage	[60]
			Gelatin methacryloyl (GelMA)	Rat bone marrow-derived stem cell	Bone	[61]
			Alginate/RGD-alginate	Human bone marrow-derived stem cell	Bone	[87]
			RGD-alginate	Human periodontal ligament stem cell/ gingival mesenchymal stem cell	Cartilage	[84]
	Microfiber	Benefits: - Homogeneous - Continuous Limitations: - Flow friction - Clogging in microchannels	Alginate	Mouse bone marrow-derived stem cell	Blood vessel	[65]
Bioprinting	Inkjet bioprinting	Benefits: - Low cost - High-throughput Limitations: - Nozzle clogging - Non-uniform droplet size	PEG-GelMA	Human bone marrow-derived stem cell	Cartilage/bone	[69]
			Type I collagen- and chitosan-agarose blends	Human bone marrow-derived stem cell	Adipose/bone	[70]
			Fibrin-collagen	Human amniotic fluid-derived stem cell and bone marrow-derived stem cell	Skin	[90]
			Agarose-collagen	Human bone marrow-derived stem cell	Bone	[86]
	Extrusion bioprinting	Benefits: - High cell density - Wide range of viscous materials Limitations: - Slow speed - Viscous liquid only	Methacrylamide gelatin	Rat bone marrow-derived stem cell	Bone	[73]
			Polylactic acid (PLA)/ GelMA	Rat bone marrow-derived stem cell	Bone	[74]
			Cellulose and alginate	Human bone marrow-derived stem cell	Cartilage	[83]
			Skin-derived ECM	Human adipose-derived mesenchymal stem cell	Skin	[89]
	Laser-assisted bioprinting	Benefits: - High cell viability - Various bioink available Limitations: - High cost	Polyester urethane urea (PEUU)	Human bone marrow-derived stem cell	Cardiac	[79]
			Plasma-alginate	Porcine bone marrow-derived stem cell	Cartilage/bone	[80]

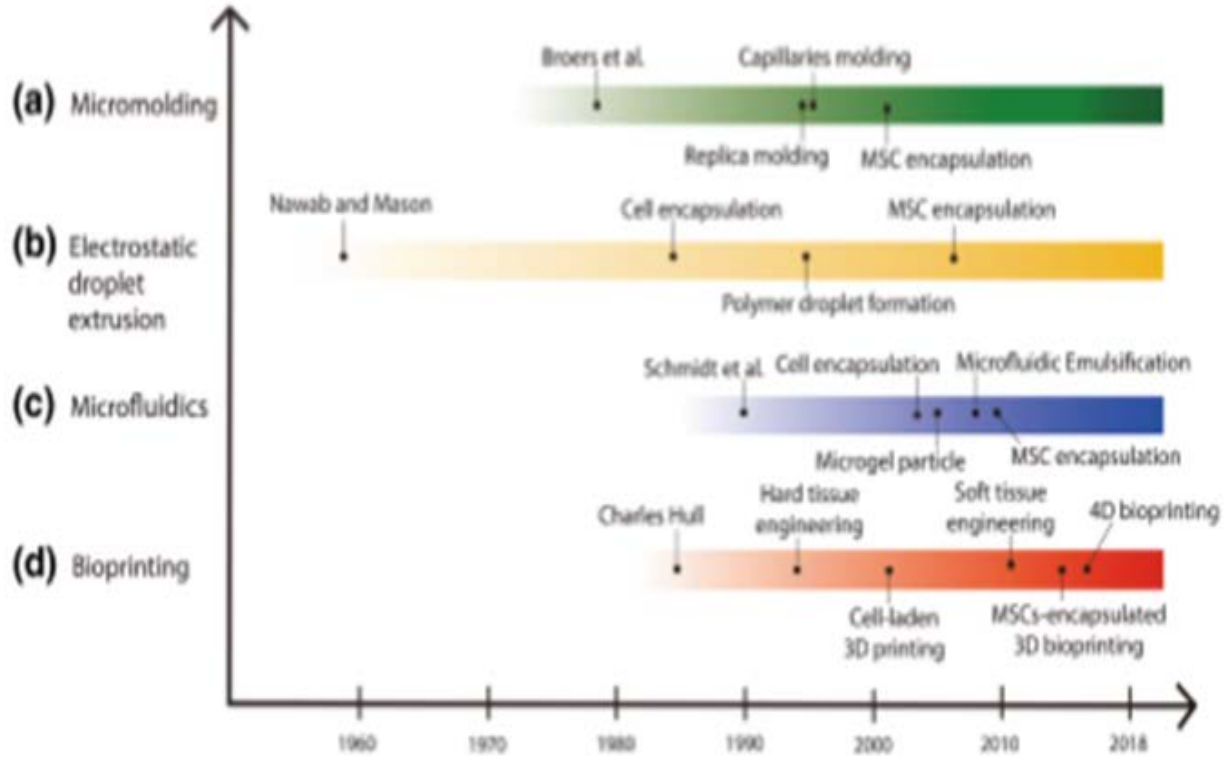

Fig. 1 Technical history and principal description of the technologies developed to achieve cell encapsulation, by year. **a** Micromolding was used in a variety of fields, but not for cell encapsulation until the early 1980s. Lithography based on micromolding was founded by Broers et al. [92] whereas techniques using replica [93] and capillary molding [94] were developed in 1996, and MSC encapsulation began in 2002. **b** Nawab and Mason suggested liquid droplets under electrostatic fields, which formed the principle of electrostatic droplet extrusion in 1958 [95]. For cell encapsulation using this technology, Goosen et al. proposed cell immobilization within a semipermeable membrane [96]. Moreover, Bugarski et al. proved the mechanism of polymer droplet formation with electrostatic droplet extrusion in 1994 [42]. Finally, MSC encapsulation was conducted in the late 2000s [97, 98]. **c** Schmidt et al. introduced a microfluidic device in 1990 [99], and the cell encapsulation was studied by Sugiura in 2005 [100]. Zhang et al. generated microgel particles with a capsular structure [101]. Microfluidic emulsification, achieved by Edd et al., offered enhanced controls over a number of encapsulated cells [102]. In 2010, MSC encapsulation was beginning to be studied. **d** The 3D printer was invented by Charles W. Hull in 1983 [103]. The inkjet 3D printing-based hard tissue scaffold was developed by Gima et al. in the early 1990s [104], which was an earlier step for application into soft tissue engineering [105]. Cell-laden and MSC-encapsulated 3D bioprinting was attempted form the 2000s onward after the development of the cell-free printed scaffold [74]. Finally, 4D bioprinting was developed as an advanced bioprinting technique for next-generation technology in the biomedical fields [106]

➢ Applications of cell encapsulation as regenerative medicine

- 세포 캡슐화 기술은 MSC를 여러 종류의 조직으로 분화시키기 위해 MSC의 생존력과 기능을 유지하기 위한 생체모방적 3D 환경을 제공하며 3D 환경은 matrix의 구성 성분, substrate stiffness, 다공성 및 substrate structure 등을 통해 MSC에 영향을 미치게 됨.

- 다양한 3D 환경은 세포 부착과 증식에 있어서 중요한 MSC와 matrix 사이의 integrin 상호작용과 clustering에 영향을 미치는데 이러한 영향은 핵에서 유전자 발현을 통제하게 되고 따라서 세포의 표현형이 달라지는 결과를 가지고 옴. 결과적으로 조직 재생은 조직의 특정 ECM parameter로 인해 조직의 종류에 맞는 환경이 필요하게 되고 MSC 분화를 증가하기 위한 생체역학적 자극이 충분하지 않기 때문에, BMP-2, TGF- β1, VEGF, FGF와 같은 성장 인자, 즉 생화학적 구성성분이 필요하게 됨.

- 3D 캡슐화 기술은 MSC와 성장인자를 같이 캡슐화함으로써 MSC에 물리화학적 영향을 제공하므로, MSC 캡슐화 기술은 target tissues에 따라 최적화시켜야 함. 다양한 조직 중에 카트리지와 뼈가 대표적으로 연구가 많이 된 단단한 조직이며 피부는 광범위하게 연구된 무른 조직이고 조직 재생에 필요한 혈과 재생 또한 중요한 관심사로 연구되고 있음.

- MSC 캡슐화 기술의 장점은 MSC의 생존력, 증식, 분화 능력을 증진시키고, 체내 면역계로부터 MSC를 보호하는 데 있고 3D 환경 구조를 포함한 이러한 기술은 결손된 특정 부분에 MSC를 안전하게 전달함으로써, 조직 재생을 위한 장기간 세포 기반 치료를 제공함.

- 조직 재생의 임상 적용에 있어서 MSC의 대량 생산과 matrix의 규모가 커져야 하는 문제, 즉, 세포 캡슐화와 이식의 비용, 시간, 일의 효율이 문제임. 뿐만 아니라, 캡슐화된 MSC를 이식한 후 면역 반응으로부터 보호하기 위한 encapsulation biomaterial 등이 고려되어야 할 주요 문제임.

- MSC의 다분화성 때문에 매력적인 세포지만, 비정상적인 조직으로 분화할 수 있다는 점을 무시하기 어렵기 때문에 예상치 못한 분화로 인한 병은 예방되어야 하고 치료할 수 있어야 함. 따라서 MSC의 비정상적인 분화와 부작용을 억제해야만, MSC 캡슐화 기술은 치료제로서 무한한 활용이 가능해지며 MSC의 캡슐화는 상황과 목적에 따라 조직 공학과 재생 치료 분야로써, 매우 유망한 기술이 될 것으로 판단됨.

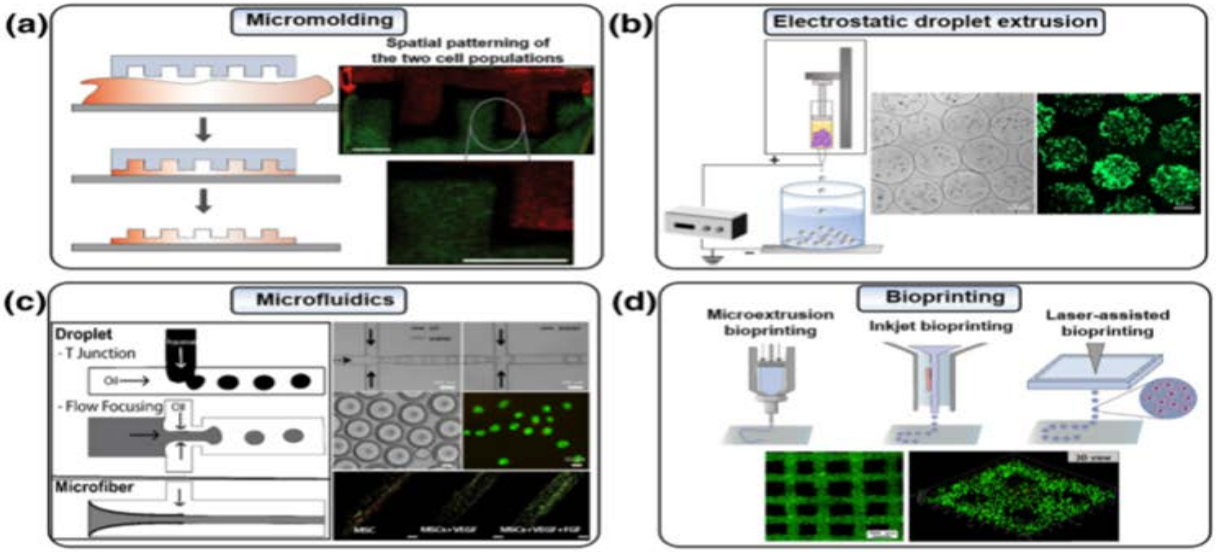

Fig. 2 MSC encapsulation technologies. The techniques for encapsulation of MSCs to maintain their viability, proliferation, and differentiation function to deliver the cells into damaged tissues in a 3D microenvironment are achieved through **a** micromolding (reproduced with permission from Reference [38]. Copyright 2013 John Wiley and Sons), **b** electrostatic droplet extrusion, **c** microfluidics (reproduced with permission from Reference [87]. Copyright 2013 Springer Nature and reproduced with permission from Reference [65]. Copyright 2017 IOP Publishing), and **d** bioprinting (reproduced with permission from Reference [107]. Copyright 2018 IOP Publishing) technologies. These technologies create various types of cell encapsulation platforms (e.g., microbeads, bulk matrices, and fiber) and specific shapes

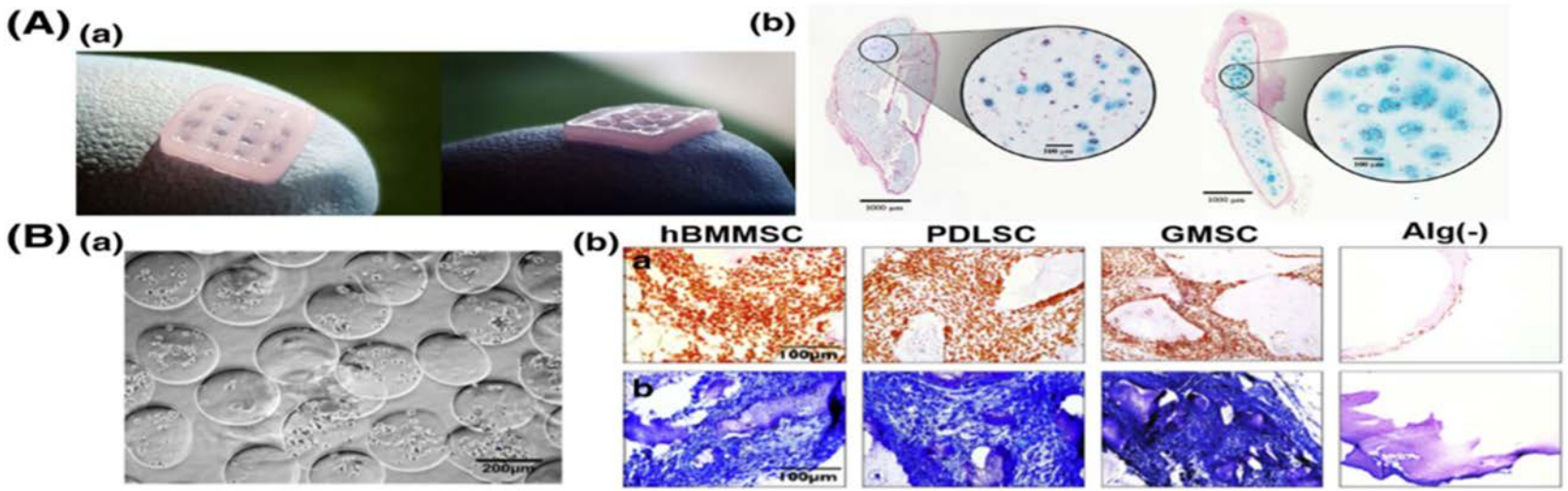

Fig. 3 Application of MSC encapsulation for cartilage regeneration. **A** (*a*) Cell-encapsulated nanofibrillated cellulose bioprinting gel. (*b*) Chondrocyte proliferation in 3D-bioprinted scaffold with hNCs and hBMSCs at day 30 (left) and day 60 (right) after subcutaneous implantation. Reproduced with permission from Reference [83]. Copyright 2017 PLOS. **B** (*a*) The periodontal ligament stem cells (PDLSCs), gingival mesenchymal stem cells (GMSCs), and hBMSC-encapsulated RGD-coupled alginate microbeads with TGF-β1 by microfluidic device. (*b*) MSC-encapsulated microbeads stained safranin-O and toluidine blue that indicates proteoglycans, significantly. Reproduced with permission from Reference [84]. Copyright 2013 Elsevier

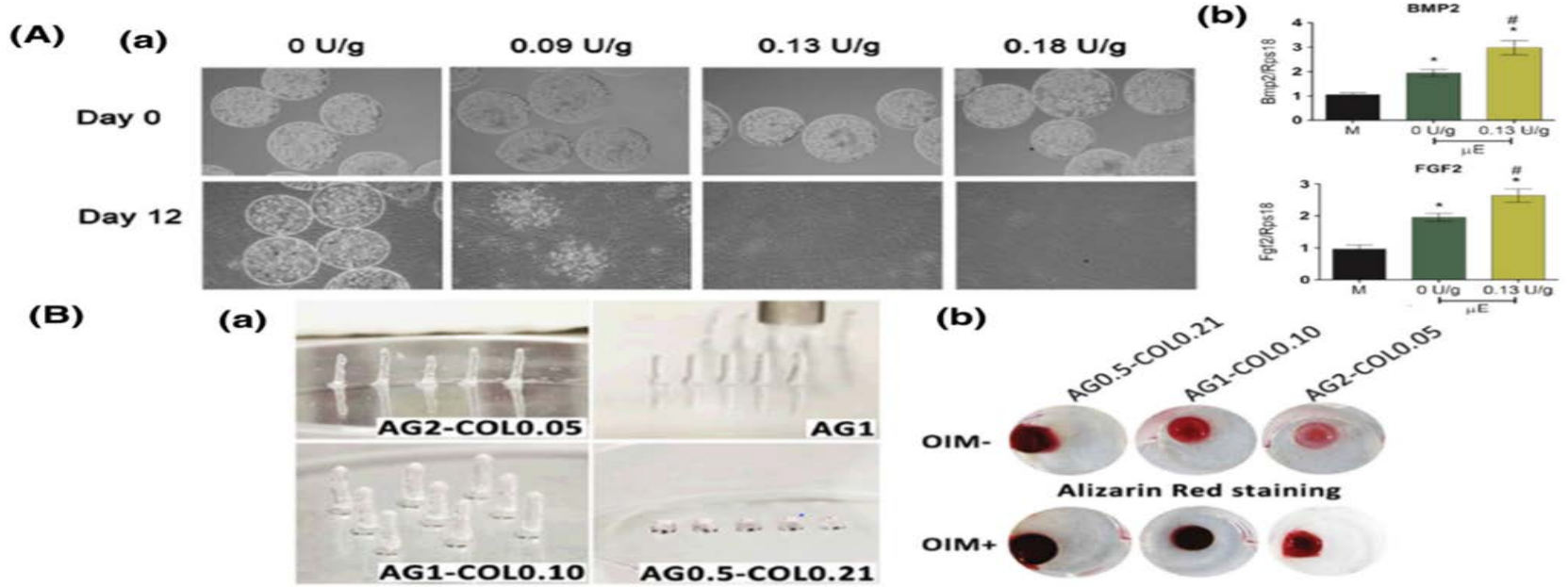

Fig. 4 Effective MSCs delivery for bone regeneration. **A** (*a*) Release of ADSCs from alginate microbeads with different concentration of alginate-lyase by electrostatic droplet extrusion. (*b*) ADSC-encapsulated alginate-lyase microbeads revealed high expression of BMP-2 and FGF-2 that regulates bone regeneration. Reproduced with permission from Reference [85]. Copyright 2013 Elsevier. **B** (*a*) Printed agarose-collagen 3D columns and rings using inkjet bioprinting. (*b*) Alizarin red staining for hBMSC-loaded agarose-collagen hydrogel scaffold. Reproduced with permission from Reference [86]. Copyright 2016 John Wiley and Sons

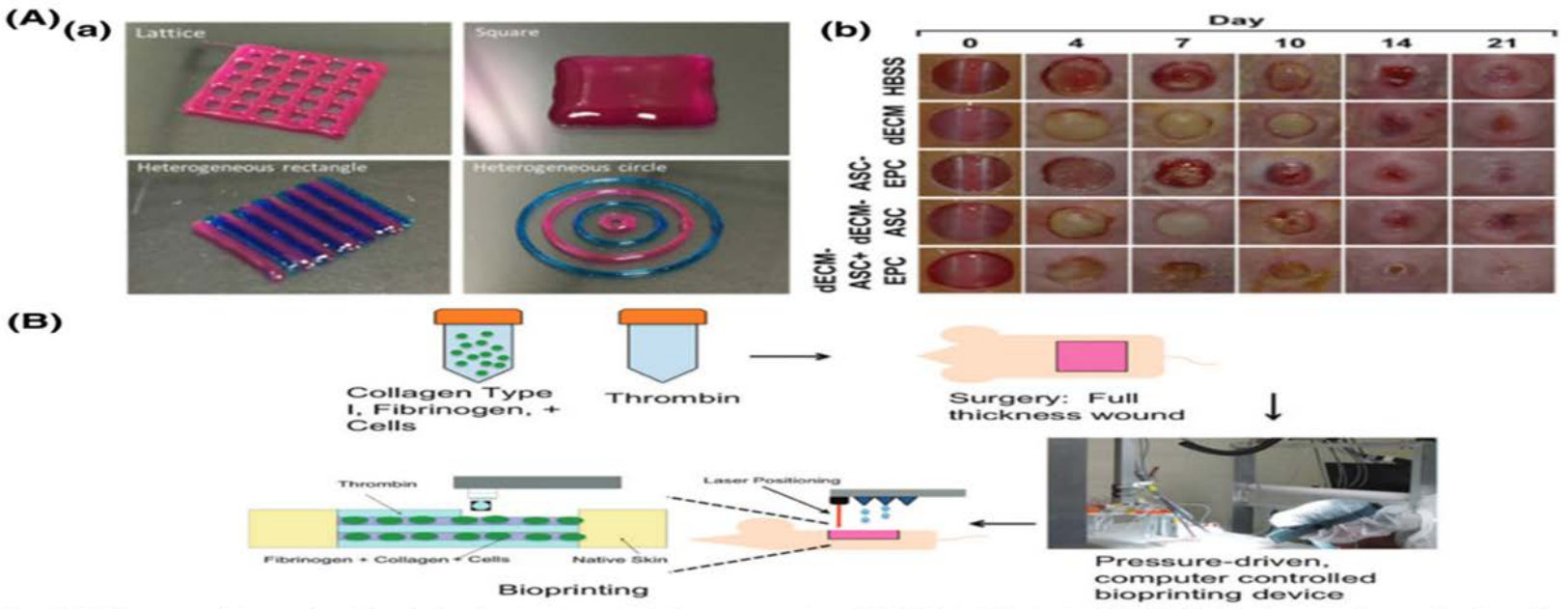

Fig. 5 MSC encapsulation using bioprinting for treatment of skin regeneration. **A** (*a*) Printability test of dECM bioink through the production of heterogeneous structure by modeling. (Bioink A: cell-free S-dECM bioink was stained with rhodamine (red); bioink B: cell-free S-dECM bioink was stained with trypan blue(blue). (*b*) The images of wound healing for 21 days. Reproduced with permission from Reference [89]. Copyright 2018 Elsevier. **B** Schematic diagram illustrating an approach to bioprinting amniotic fluid-derived stem (AFS) cells to increase the healing of full-thickness skin wounds. Reproduced with permission from Reference [90]. Copyright 2012 John Wiley and Sons

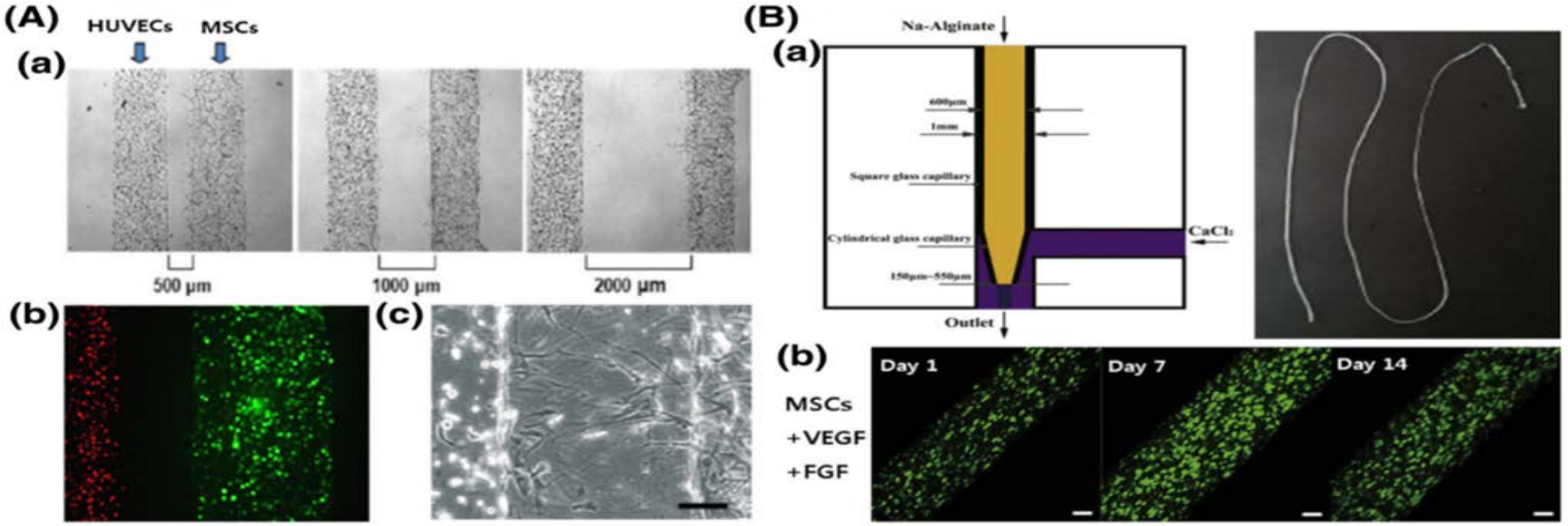

Fig. 6 Blood vessel regeneration by MSC encapsulated 3D construction. **A** (*a*) The 3D co-culture system of mesenchymal and endothelial cells in the micropatterned hydrogel. HUVEC- and MSC-loaded micropatterned fibrin channels with the distances between channels of 500, 1000, and 2000 μm. (*b*) Encapsulated HUVECs (left channel: red) and MSCs (right channel: green). (*c*) MSCs sprouted to HUVEC with distance-dependent response (scale bar,100 mm). Reproduced with permission from Reference [36]. Copyright 2009 John Wiley and Sons. **B** (*a*) Schematic diagram of microfiber generation and principle of gelation and actual shape. (*b*) MSCs with VEGF and FGF were effective for angiogenesis in microfiber over 14 days. Scale bar, 200 μm. Reproduced with permission from Reference [65]. Copyright 2017 IOP Publishing

✓ Bioinks and bioprinting technologies to make heterogeneous and biomimetic tissue constructs[4]

- 조직은 여러 다른 세포들, 세포 외 골격 물질 (extracellular matrix materials), 생체 분자로 이루어진 복잡한 구조를 가지고 있어 적절한 생체 재료의 부족과 기술의 한계로 기존의 조직공학적인 방법으로는 생체모방적이고 복잡한 조직을 완벽히 재현할 수 없었음.

- 최근, 3D bioprinting 기술의 발달로 조직 복구에 큰 발전을 이룰 수 있게 되었는데 이러한 주요 요인은 다양한 생체 재료, 다른 타입의 세포, 가용성 인자 (soluble factors) 등으로 구성된 다양한 성분을 가지는 bioink 개발이 중요한 기술임. 이러한 다양한 성분과 이종 바이오 잉크를 one-step manner로 제조되는 직접 프린팅 접근법이 최근 중점을 두고 있는 기술개발임.

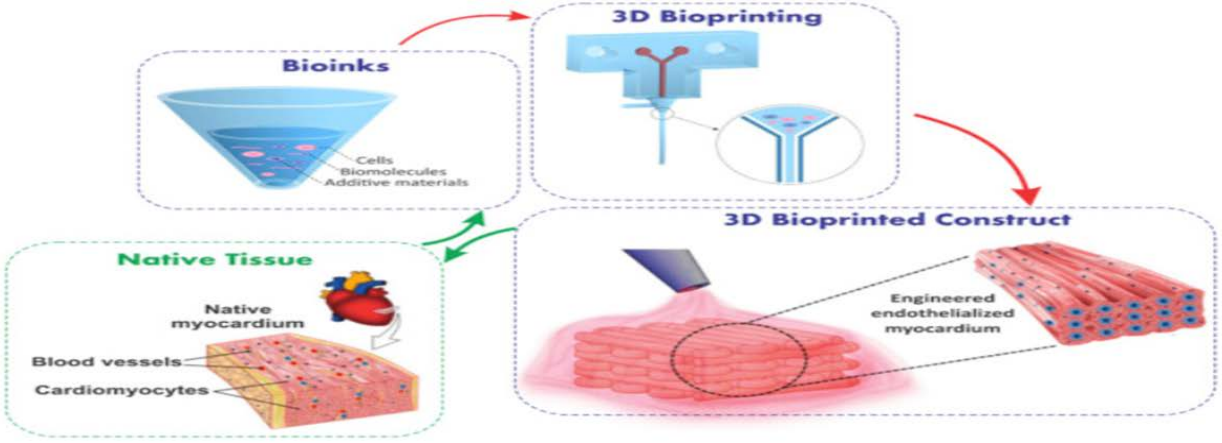

Download : Download full-size image

Fig. 1. Schematic representation of the procedure for design and biofabrication of tissue constructs from bioinks mimicking the native tissue parts of figure are reproduced from Zhang et al. [20] with permission from Elsevier.

➢ Multicomponent bioinks

- 단일 생체 재료로 만들어진 bioink는 일반적으로 생체 모방 조직과 유사한 구조물을 만드는데 필수적인 기계적 및 기능적 요구 사항을 충족시키지 못함. 보고된 바에 의하면, PEG와 같은 생체 물질은 다양한 분자량과 물리적 가교 특성의 제어가 가능한 반면 젤라틴과 피브린과 같은 세포 친화적이고 자연적인 생체 재료는 기계적 성질이 약하여 bioink로써 사용하는데 문제가 많아서 하나 이상의 재료로 구성된 다양한 성분을 가지는 bioink는 성능이 개선된 3D 바이오 프린팅에 적절하여 구조물 형성이 개선됨.

- 간단한 혼합, 공정 후 코팅 (postcoating), 화학적 가교를 포함하여 다른 생체 재료의 혼합방법을 보여주고 있으며 구성 재료에 기초하여 분류하여 다음과 같이 설명하고 있음.

1. Bioinks having combination of natural materials: 다음과 같이 두 종류의 natural materials을 혼합한 bioink는 지지체로써 기계적 특성이 향상됨으로써 세포의 부착력이나 생존력이 향상됨.
   - ▶Alginate with gelatin/fibrin:
   - ▶ Silk fibroin with gelatin:
   - ▶ Agarose with collagen
   - ▶ Chitosan with gelatin
   - ▶ Cellulose with alginate
   - ▶ Hyaluronan with cellulose

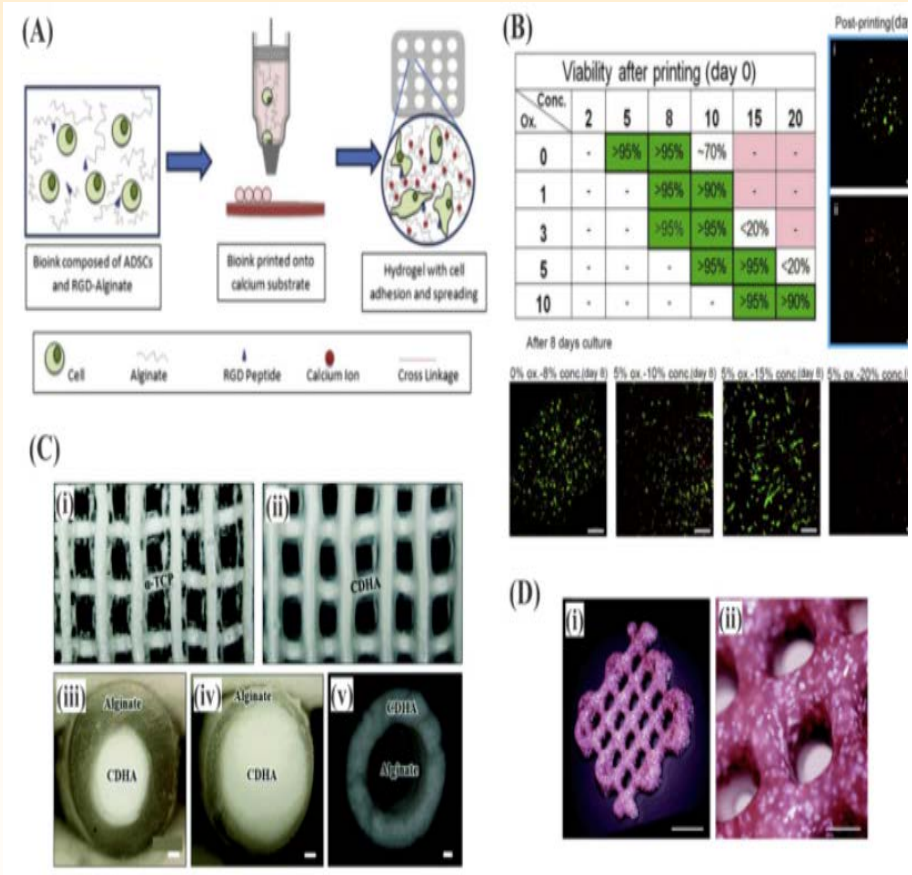

Fig. 3. (A) Schematic illustration of droplet-based fabrication process for lattice structure made of human adipose tissue–derived stem cells encapsulated in alginate and (B) the resulting cell viability as a function of bioink parameters. Alginates with medium viscosity resulted in higher cell viability owing to limited nutrition transfer at high and low concentrations. Reproduced from Jia et al. [48] with permission from Elsevier. (C) Representation of 3D printed alpha tricalcium phosphate (α-TCP)/alginate core/shell scaffolds (i) before and (ii) after crosslinking, (iii-iv) fiber cross sections demonstrating the core/shell structure of alginate and calcium-deficient HAp. Scale bar = 100 μm. Reproduced from Raja et al. [49] with permission from the Royal Society of Chemistry. (D) Three-dimensional printing of a porous scaffold consisting of alginate, mesenchymal stem cells and, calcium phosphate particles using extrusion printing. Scale bar = 500 μm. Reproduced from Loozen et al. [50] with permission from the Royal Society of Chemistry. Hap, hydroxyapatite; RGD, Arg-Gly-Asp.

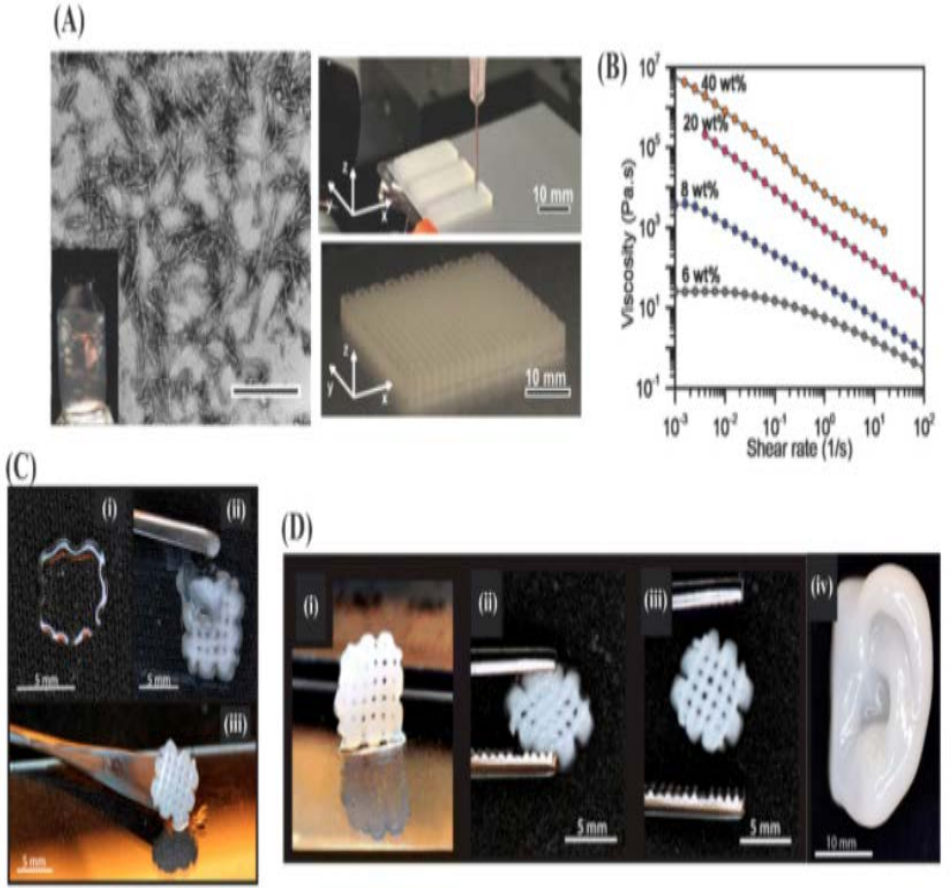

Fig. 4. (A) Wood pulp CNC distribution in the aqueous inks (scale bar = 500 nm) and photograph of the printed cellular constructs based on CNC inks. (B) Shear-thinning was induced to the ink slightly at 1% CNC concentration and increased significantly at around 10–20% as the viscosity decreased with shear rate. Reproduced from Siqueira et al. [65] with permission from Wiley-VCH Verlag GmbH & Co. (C) The printed constructs for a grid design obtained by using (i) 3% alginate, (ii) 2.5% NFC, or (iii) alginate/NFC inks. Combining the inks resulted in successful and structurally integrated (fully cured) constructs. (D) (i-iii) Mechanical recovery of the meshes and (iv) human ear model obtained by the use of alginate/NFC inks. Reprinted from Markstedt [67] with permission from the American Chemical Society. CNC, cellulose nanocrystals; NFC, nanofibrillated cellulose.

2. Bioinks comprising natural and synthetic components: 향상된 생체적합성, 기계적 성능, 열적 특성, 가교성을 갖는 생체 재료를 천연 재료와 합성된 재료를 조합하여 개선점을 얻을 수 있음. 많은 연구에서 합성 생체 재료를 천연재료와 함께 사용하여 bioink를 개발함.

3. Bioinks comprised of synthetic biomaterials: PEG는 수용성이며 순수한 PEG는 3D 바이오 프린팅에 적합하지 않은 물질이지만 bioink로 사용하기 위하여 poly(ethylene glycol) diacrylate (PEGDA) 또는 methacrylate (PEGMA) 과 혼합하여 개발한 결과 조골 세포와 같은 세포가 캡슐화 될 수 있고 PEGMA와 같은 PEG 생체 물질 내에서 세포가 잘 생존 할 수 있다는 것을 입증함.

4. Bioinks comprised of hydrogels and particles: 첨가된 나노 물질은 고분자 사슬을 고정시키고 하이드로 겔의 기계적 강도를 향상시키기 위해 가교제로 사용될 수 있음이 보고되고 있어 3D 바이오 프린팅된 구조물의 기계적, 화학적, 전기적 특성을 조절하기 위해 나노 입자를 첨가하여 bioink 재료인 생체 재료 개발에 대한 많은 연구가 보고되고 있음.
   - Silicates
   - Hydroxyapatite
   - Tricalcium phosphate
   - Bioactive glass
   - Carbon nanomaterials

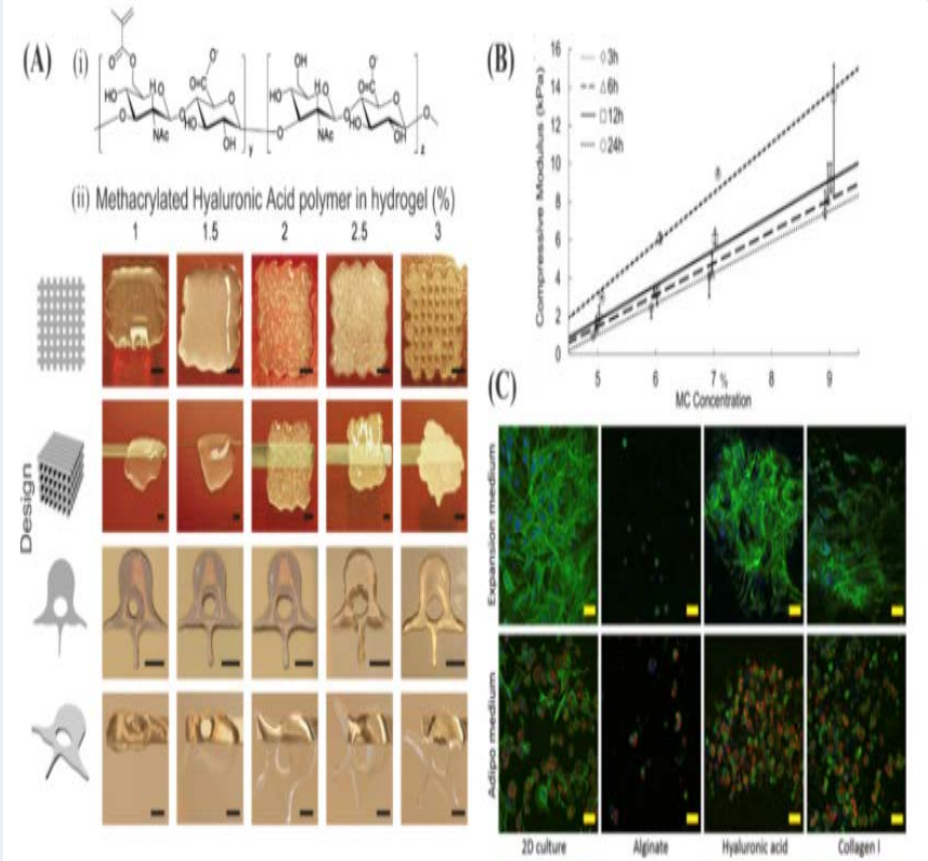

Fig. 5. Characteristics of printed constructs based on HA modified inks. (A) (i) Chemical structure of methacrylated HA obtained by reacting HA with methacrylic anhydride in an aqueous environment and (ii) printability of methacrylated hyaluronic acid (MeHA) at different concentrations (scale bar = 500 μm). The best printability was attained at MeHA concentration of 3%. Reproduced from Poldervaart et al. [71] (B) Compressive elastic properties of HA methylcellulose as a function of methylcellulose at different time points. Reproduced from Law et al. [74] with permission from Elsevier. (C) Comparing cell response in two different culture media (expansion and adipo), for cells seeded on either 2D surface or encapsulated in alginate, HA, or in collagen gels. Promoted cell differentiation and proliferation were seen in HA and collagen I gels (scale bar = 50 μm; nuclei, actin filaments, and lipid droplets were shown in blue, green, and red, respectively). Reproduced from Henriksson et al. [75] with permission from IOP Publishing Copyright 2016. HA, hyaluronan.

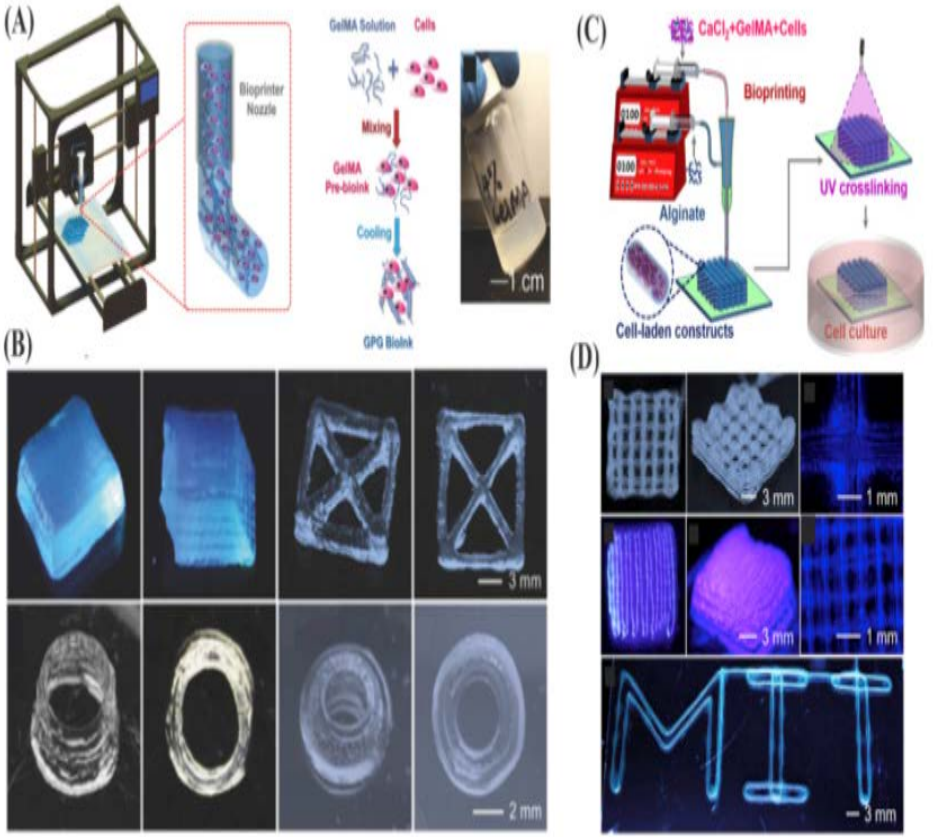

Fig. 6. (A) 3D bioprinting of bioinks composed of cells and GelMA. (B) Low concentration 3D GelMA structures were fabricated by taking advantage of shear-thinning properties of GelMA, i.e. cooling down the structures to maintain their structural integrity. Reproduced from Liu et al. [78] with permission from WILEY-VCH Verlag GmbH & Co. (C) Illustration of GelMA/alginate microfibers with core/sheath architecture forming bioprinted constructs through extrusion 3D bioprinting. (D) Alginate sheath allows printing of 3D structures using low concentration GelMA (lower than 2%). Reproduced from Liu et al. [76] with permission from IOP Publishing. GelMA, gelatin methacryloyl.

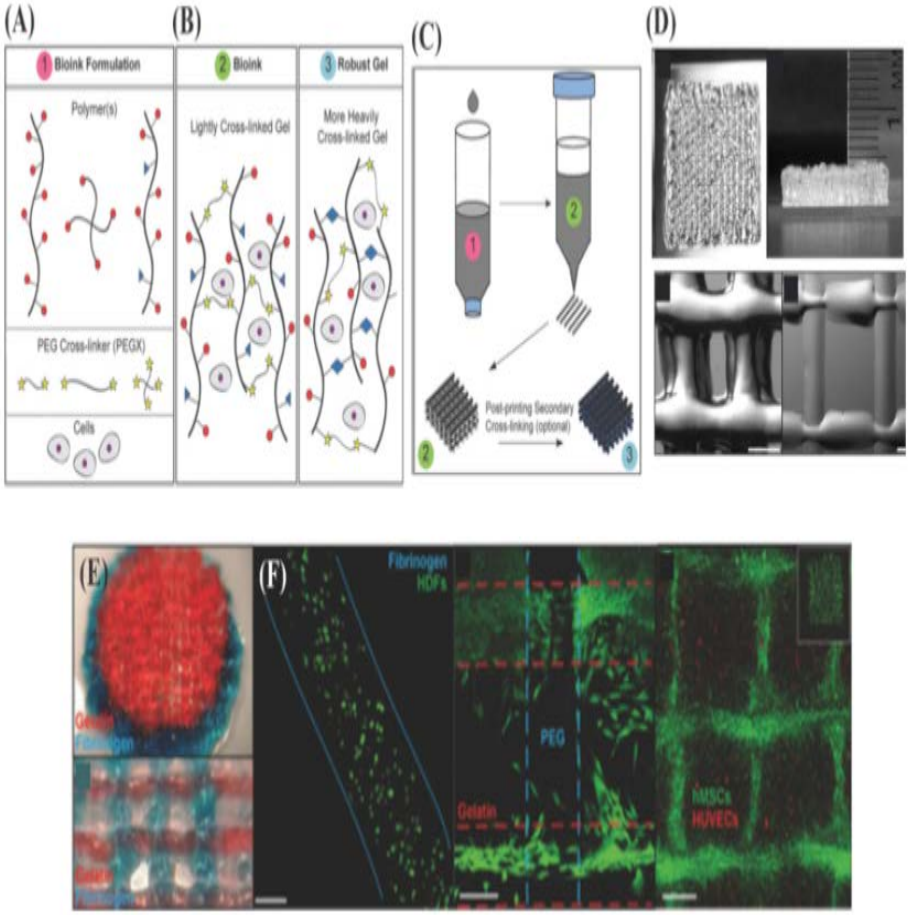

Fig. 7. (A) Different types of polymer chain, crosslinker, and cells for developing cell-incorporated inks based on PEG. (B) Ink configuration after lightly and heavy crosslinking of PEG. (C) Three-dimensional printing strategy of developed PEG ink. Secondary crosslinking may be applied for heavily crosslinking the polymer chains after the 3D printing process was completed. (D) Photograph of 3D printed structures using PEG-gelatin bioinks (scale bar = 500 μm). (E) Examples of combined 3D bioprinting of PEG-gelatin (red) and PEG-fibrinogen (blue) bioinks in spheroidal and grid designs and (F) cell viability results associated with using 3 w/v% fibrinogen in PEG, PEG-PEG, and PEG-gelatin (scale bar = 200 μm). Human umbilical vein endothelial cells (HUVECs) seeded with human MSCs, which filled the pore spaces in the internal structure. Reproduced from Rutz et al. [87] with permission from WILEY-VCH Verlag GmbH & Co. PEG, polyethylene glycol; MSC, mesenchymal stem cell.

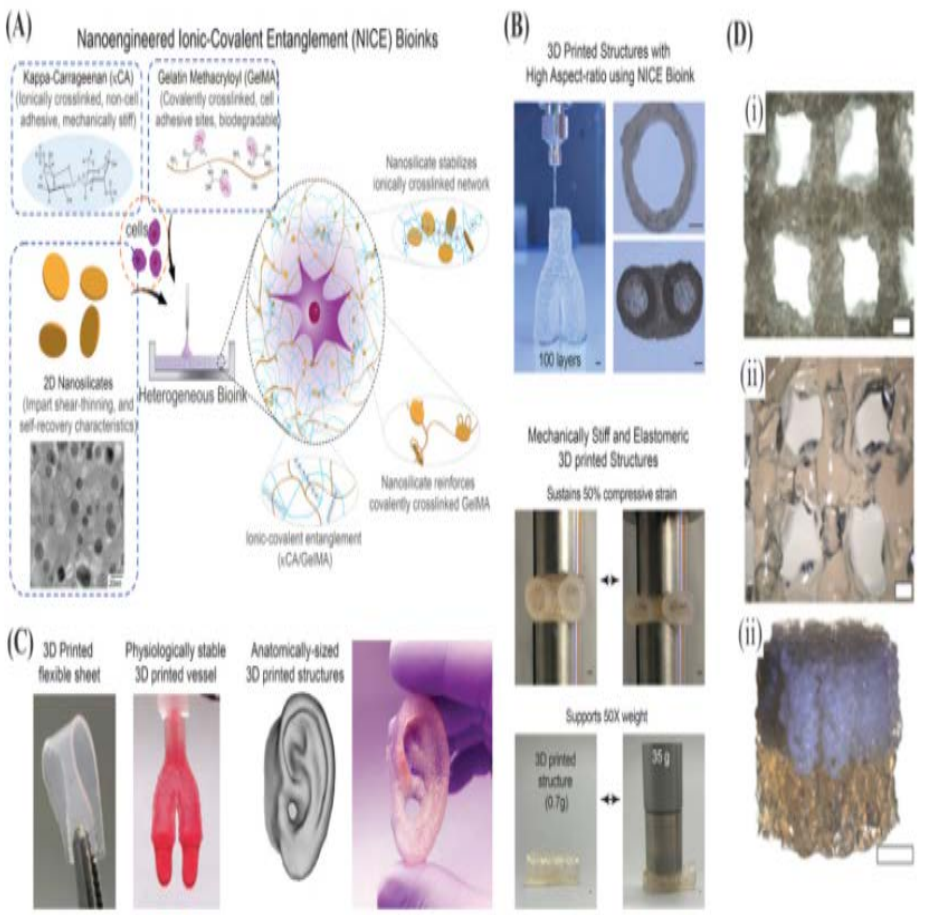

Fig. 8. (A) Nanoengineered ionic-covalent entanglement (NICE) bioinks developed by taking advantage of nanoparticle ingredients: (1) Kappa-Carrageenan (κCA) for ionic crosslinking, (2) GelMA for covalent crosslinking, tissue adhesion, and biodegradability, and (3) 2D nanosilicates for having shear-thinning properties. (B) The NICE-based printed constructs exhibit promising mechanical recovery behavior (scale bar = 1 mm). (C) High printing fidelity was achieved by the NICE ink because of versatile printing of complex 3D structures and human organs. Reprinted with permission from Ref. [92]. Copyright 2018 American Chemical Society. (D) Porous constructs fabricated by gelatin methacrylamide-gellan gum MSC-laden bioinks: (i) MSC-laden layer (scale bar = 400 μm), (ii) GelMA-gellan gum layer (scale bar = 400 μm), and (iii) perspective photograph of the bilayered GelMA-gellan gum cylindrical osteochondral graft model (scale bar = 4 mm). Reproduced from Levato et al. [91] with permission from IOP Publishing. GelMA, gelatin methacryloyl, MSC, mesenchymal stem cell.

5. Bioinks for 4D printing: 4D 바이오 프린팅을 통해 외부 자극의 유무에 관계없이 시간이 지남에 따라 모양이나 기능이 변할 수 있는 조직 구조물을 만들 수 있는 bioink 개발을 보고하고 있음. 온도, 전기장, 자기장, 습도와 같은 외부 자극에 반응하여 변형되는 물질 개발에 대한 연구들이 보고됨.

6. Multicellular and stem cell–based bioinks: 천연 조직은 일반적으로 다른 유형의 세포로 구성되기 때문에, 생체모방 지지체를 만들 때 다른 유형의 세포들을 고려하여야 하며, 3D 바이오 프린팅을 위한 적절한 세포의 선택은 만들어진 지지체 구조물에서 조직화 하는데 매우 중요함.
   - ▶ Dynamic hydrogels for multicellular 3D bioprinting

7. Biomolecule-contained bioinks: 3D 구조물에서 세포 기능을 조절하기 위해서는 생체 분자가 필요하여 다음과 같은 생체 분자 방출 특성을 갖는 구조물이 개발됨.
   - ▶ Bone morphogenetic proteins
   - ▶ Vascular endothelial growth factor
   - ▶ Fibroblast growth factor
   - ▶ Transforming growth factor
   - ▶ Stromal cell–derived factor
   - ▶ Extracellular matrix
   - ▶ Peptide motifs
   - ▶ Platelet-rich plasma
   - ▶ Stem cell secretomes and other molecules

- Methods to fabricate heterogeneous constructs: 성공적인 생체 모방, 이종 구조물을 개발하기 위해서는 적절한 제작 도구와 방법이 필요하여 각 기술의 시스템을 다음과 같이 보고하고 있음.

  - Multihead systems
  - Core-shell needle system
  - Stereolithography
  - Digital light projector
  - Multimaterial microfluidic bioprinting

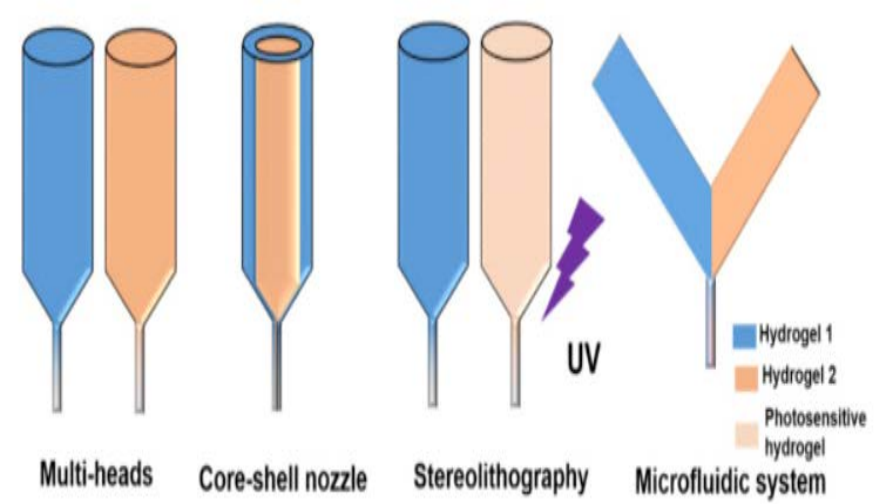

Fig. 11. Schematic illustration of different 3D printing systems that have been used to produce multimaterial constructs.

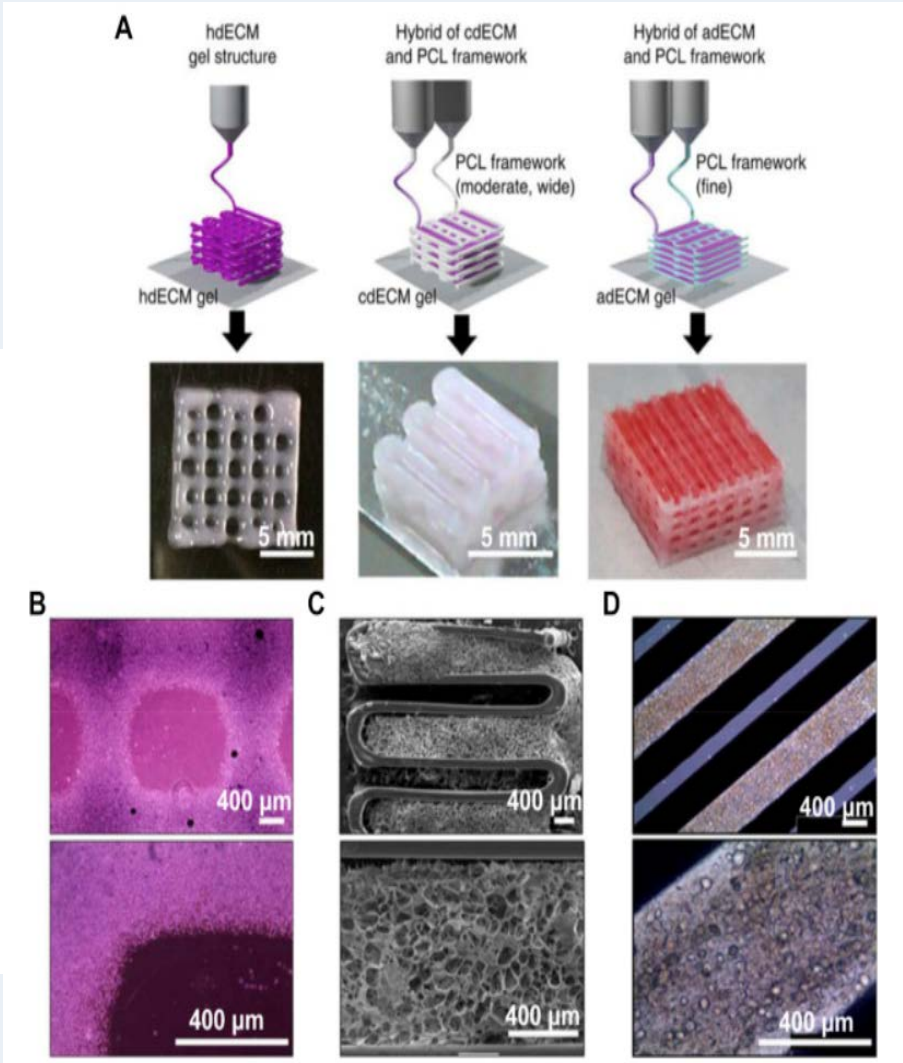

Fig. 12. Three-dimensional printing with (A) single and (B, C, and D) multiprint head systems [175]. PCL, poly(ε-caprolactone); dECM, decellularized ECM

➢ 3D printing for tissue engineering application[5]

- 조직공학의 목표는 재생 치료나 전체 장기 이식을 목적으로 기능적인 조직이나 장기를 만드는 것임. Bioprint된 조직은 조직공학이나 재생 의학 분야에서 가장 매력적인 방법이고 Bioprint에 의해 만들어진 복합 구조 제작에는 layer-by-layer 제작 방법이 필요함.

- Bioprinting을 통해 지지체와 조직을 제작하기 위해선 3가지 과정을 기반으로 진행됨.
  1. 이미징 작업과 컴퓨터를 통해 print하고 싶은 조직의 디자인을 설계
  2. 적절한 재료의 bio-ink를 생산
  3. 지지체나 조직을 만들기 위한 적절한 bioprinter 선택

- 3D bioprinting 기술에 대한 접근방식은 생체모방, 자율적 자가 조립 (autonomous self-assembly), mini-tissue building blocks 등이 보고되고 있으며 조직 공학 및 재생 의학을 위한 3D 프린팅의 현재와 미래의 잠재적 응용에 대해 보고하고 있음.

- 자율적 자가 조립은 조직을 복사하는 수단으로 배아줄기세포로 만든 장기 개발을 이용하는 접근법임. 개발된 조직의 초기 세포구성 성분은 extracellular matrix (ECM)의 성분, 적절한 세포 신호, autonomous organization, 그리고 원하는 생물학적 micro–architecture로 만들어진 패턴과 기능에 의해 만들어짐. 미니 조직의 기본 구성은 생체모방, 자가 조립 방법과 관련 있으며. 디자인 및 자가 조립에 의한 미니 조직은 더 큰 구조를 제작하고 조립할 수 있음.

➢ IMAGING & DESIGNING TISSUES

- 기능적 조직이나 장기를 프린트하기 위해선 모델링을 정확하게 하는 것이 중요하며 의료용 3D 시각화 기법은 실제적인 규모이면서 세부적으로 장기를 시각화하는 정확도에 중요함.

- 의료 분야의 시각화 기술은 3D에 대한 구조에서의 data와 세포, 조직, 장기, organism level 기능을 제공하며 CAD (Computer Aided Design)와 컴퓨터 보조 제조 도구는 조직과 장기에 대한 복잡한 구조 정보를 수집하고 디지털화 함.

- 자기공명영상 (MRI)과 컴퓨터 단층촬영 (CT)과 같은 많은 최신 영상 및 진단 기술은 대상 조직에 대한 정보를 획득하고 이식물의 CAD 데이터를 얻기 위해 이용되고 있음.

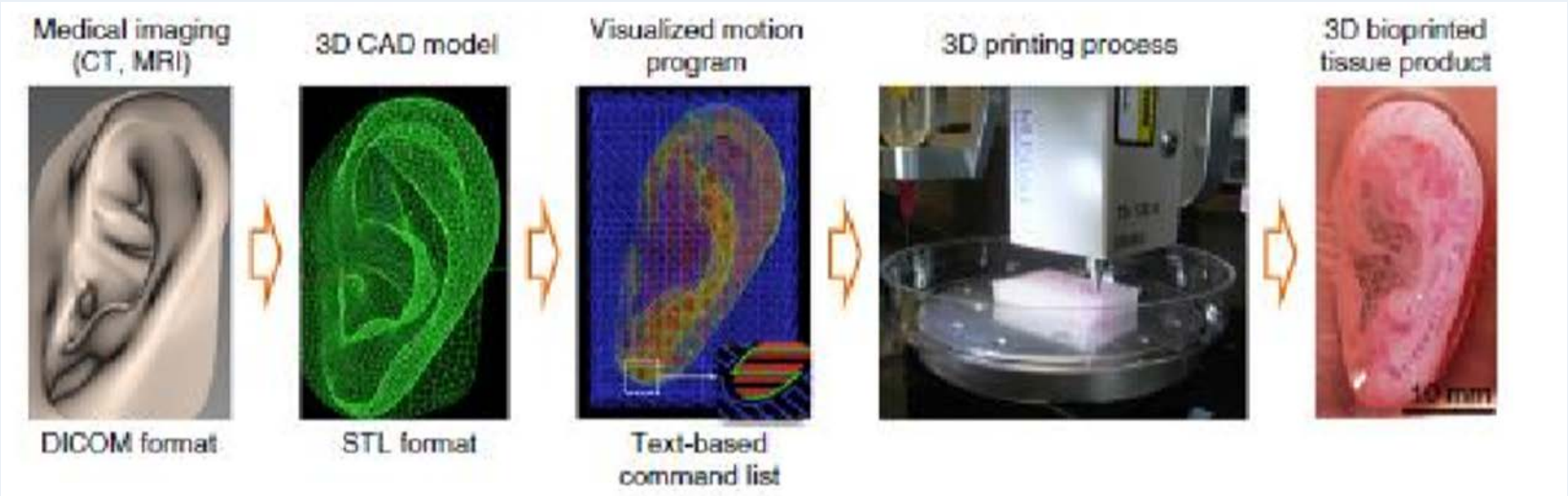

Figure 1. Modelling tissue for 3D printing [6].

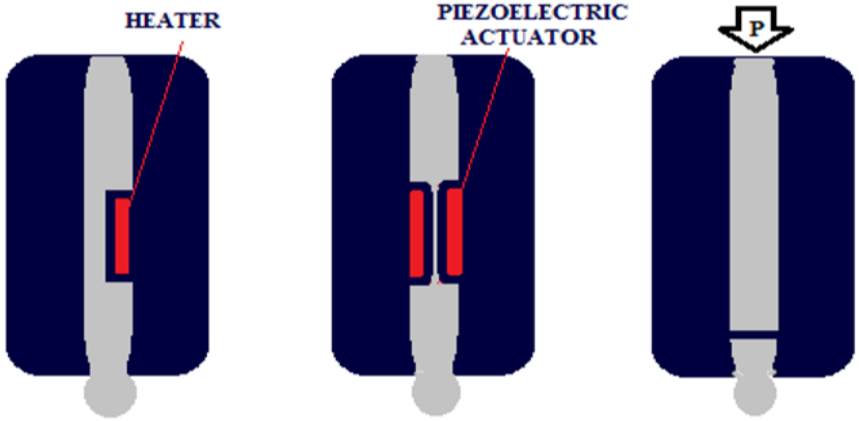

Figure 2. Schematic representation of inkjet printer methods. The figure on the left shows thermal inkjet bioprinter. The figure in the middle shows piezoelectric bioprinter. The figure on the right shows mechanical inkjet bioprinter

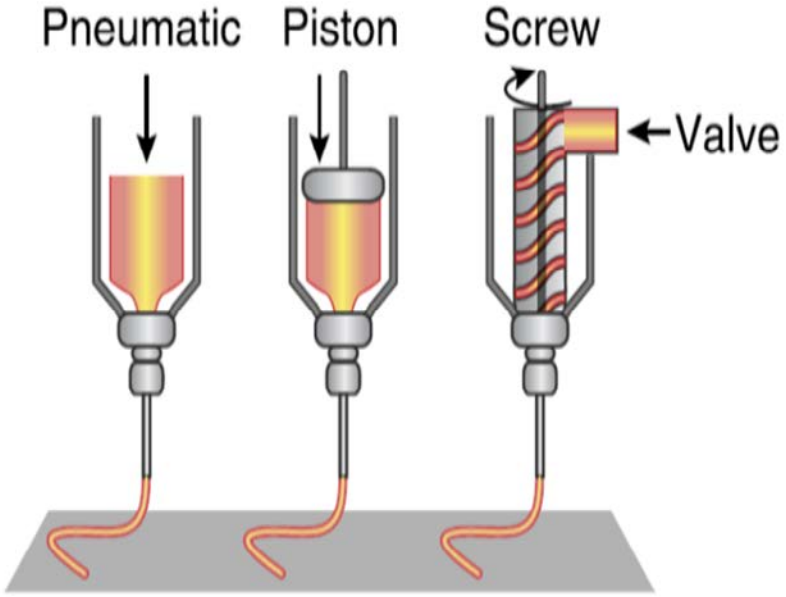

Figure 3. Microextrusion bioprinting systems [2].

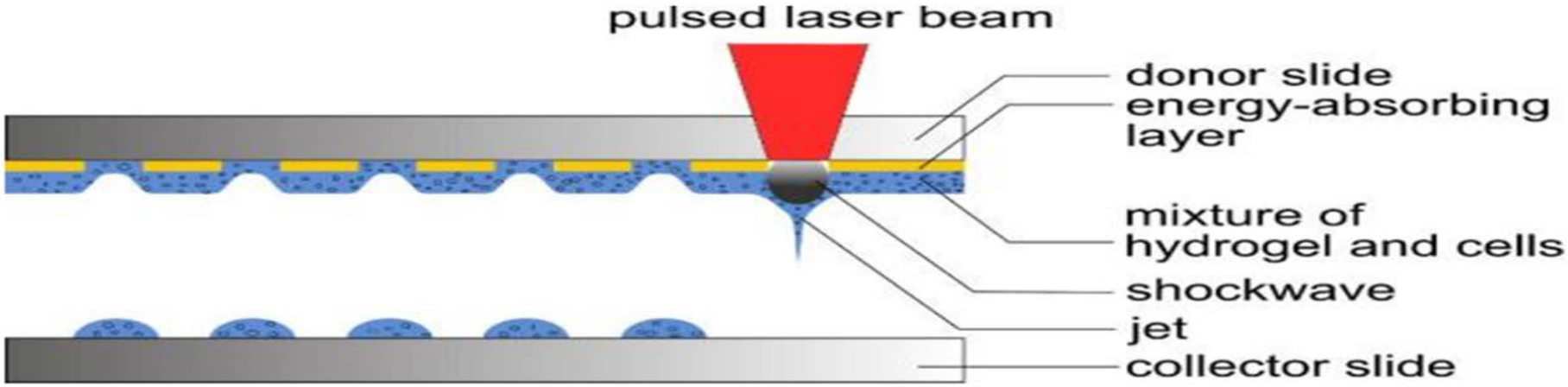

Figure 4. Schematic laser-assisted bioprinting setup [17].

➢ MATERIALS & BIOINK

- Bioink printing 방법은 두 가지
  1. bioink를 다양한 폴리머로 이용하여 기능성 지지체로서 프린트하는 방법
  2. 세포를 오직 bioink 재료로 사용하여 지지체 없이 프린트하는 방법

- 두 경우 모두, 세포가 포함된 bioprint된 구조물은 혈관 구조를 모방하거나 다공성을 통해 충분한 영양 전달이 필요하며 프린트된 물질은 구조를 물리적으로 지지해야 하므로 지정된 조직이나 위치에 적합한 기계적 특성을 가져야 함.

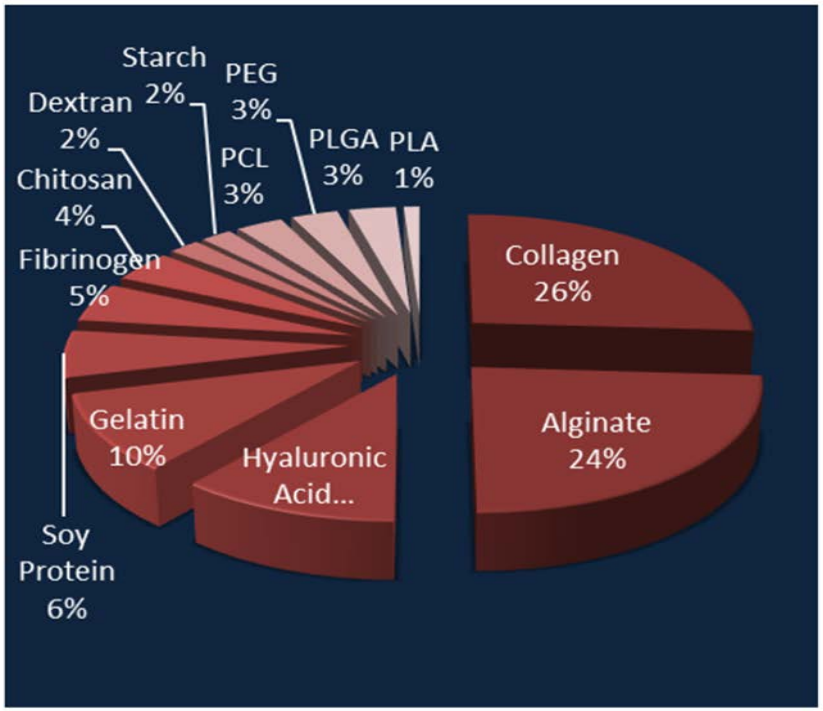

Figure 5. Chart diagramming natural and synthetic polymer distributions for use as bioinks compiled from relevant literature [19].

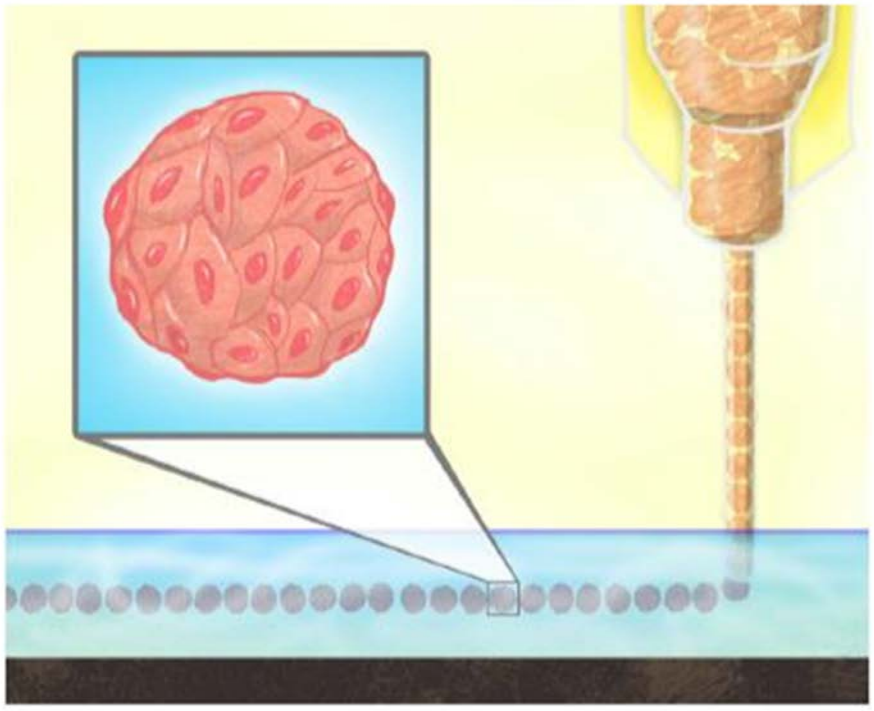

Figure 6. Spheroids are printed into ''biopaper'' which is a layer of hydrogel [23].

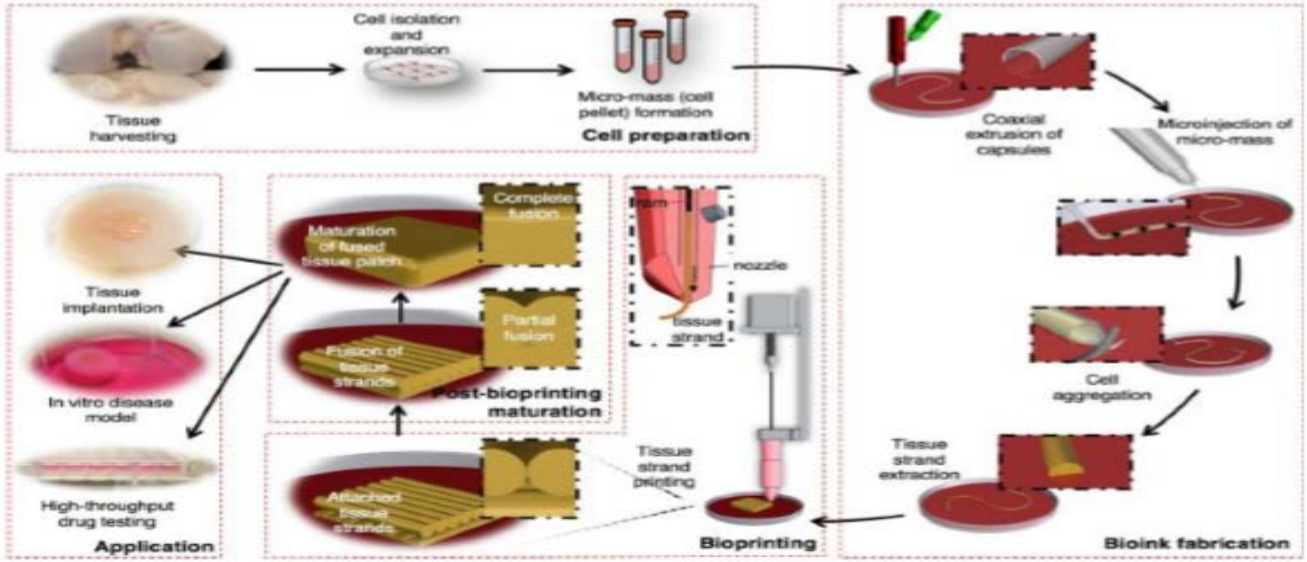

Figure 7. The concept of tissue printing using tissue strands as bioink [26].

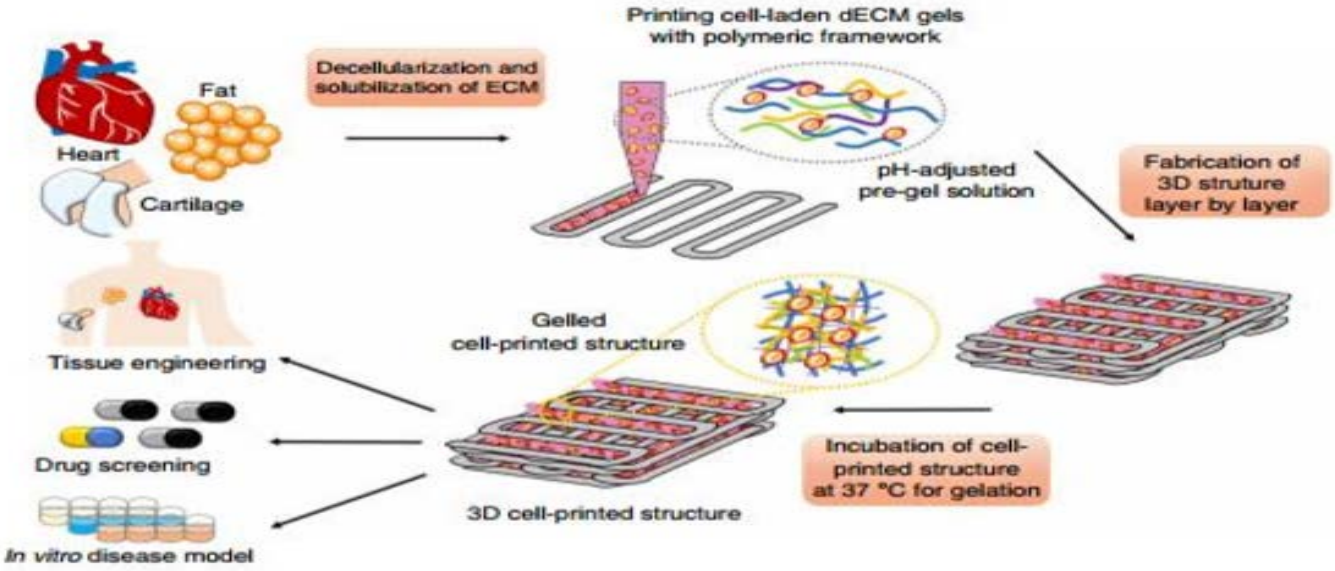

Figure 8. Schematic procedure for dECM bioink bioprinting [27].

Table 1. Biocompatible polymers used as bioinks for stem cell, cell delivery, and scaffold materials are presented along with their crosslinking features and application in bioprinting stem cells [20].

BIOINK	PROPERTIES	CROSSLINKING FEATURES	EXAMPLES
ALGINATE	Inexpensive, natural polysaccharide derived from algae. Bioinert, which may lead to anoikis and is often modified with RGD or additives such as hydroxyapatite.Crosslinking occurs rapidly hence alginate is very popular as a bionk.	Instant gelation in Ca^{2+} solution.	Fabrication of osteochondral tissue equivalents.
AGAROSE	Bioinert. Forms cytocompatable and structurally stable hydrogels. Solidifies slowly, resulting in bioink spreading. Not biodegradable in mammals.	Thermal gelation, cells mixed at 40 °C and gelates at 32 °C. No other polymerizers needed.	Printing of bone marrow stromal cells in agarose has been assessed.
HYALURONIC-MA	A non-sulfated glycosaminoglycan, usually used for producing soft tissue like hydrogels rather than ones confering structural stability. Often mixed with gelatin, dextran or other polymers to overcome bioinertness and mechanical weakness.	UV triggered free radical polymerization.	Adipose stem cells printed in Gel Ma/HA Ma hydrogel, confering high cell viability detected after 1 week (97%).
FIBRIN	Natural protein comprised of cross-linked fibrinogen, has quick crosslinking rate and is glue like in form. The mechanical stiffness is low, so often used in conjunction with other polymers.	Crosslinks through the thrombin cleavage of fibrin.	Blended with collagen to deliver stem cells by inkjet with the application of skin regeneration.
SILK FIBROIN	Good biocompatability and mechanical properties. Mixed with gelatin to prevent nozzle clogging.	Crosslinked with tyrosinase or by sonification.	Silk fibroin-gelatin bioink used to print human nasal inferior turbinate tissue derived MSC that supports multi lineage differentiation.
GELATIN	Formed from partially hydrolysed collagen. More soluble than collagen. Melt/gelation temperature 30 °C–35 °C, requires secondary crosslinking for applications at physiological temperatures. Matrix can be remodelled by cells.	Crosslinked using gluteraldehyde, carbodimiide or transglutaminase. UV irradiation of the methycrylated form.	BMSCs printed in gelatin MA with BMP2 or osteogenic medium.
COLLAGEN-I	Rich in the intergrin binding RGD motif. The ionic or pH changes involved in gelation are usually not gentle enough to allow cell bioprinting, however water soluble forms do exist. Collagen hydrogels are formed at low concentration. That confer for low elastic modulus. Unfortunately a 100% collagen hydrogel may not be ideal as a cellularized construct due to water exclusion and contraction induced by hydrophobic peptide residues.	Gels through hydrophobic bonding with a slow rate of crosslinking, so can be blended with faster crosslinking polymers such as alginate or fibrin.	MSCs in collagen hydrogel differentiate towards chondrocytes, expressing cartilage proteins.
dECM	Supplies a natural like ECM niche for the stem cells. The stem cells seeded in dECM scaffold show greater degree of differentiaiton than cells seeded in collagen.	Can form a bioink that remains as a solution below 15 °C and gels after 30 min at 37 °C.	Adipose, cartilage, and heart dECM used as cell printing bioink for adipose derived SCs and human inferior turbinate tissue derived MSC.
MATRIGEL	ECM like hydrogel rich in laminin, collagen and heparan sulfated proteoglycan. Has been used extensively for 3D cell culture.	Thermal gelation.	Not widely employed for bioprinting, used for printing HepG2 cells by temperature comtrolled syringe.
METHYL CELLULOSE	Can be used to aid printing of another polymer and is then released. Enhances print viscosity and porosity following release.	Thermal gelation.	Blended with alginate to print MSCs into a low concentration alginate hydrogel.
PEG	Bioinert, variable molecular weight allows tunable properties, altering stiffness can aid stem cell differentiation. Can easily joined to other molecules. Requires modification to allow crosslinking.	UV initiated photocrosslinking of the PEGDMA.	Bone marrow derived MSCs printed for osteogenic and chronogentic differentiation.

참고 문헌

1. Development of an Anti-Inflammatory Drug-Incorporated Biomimetic Scaffold for Corneal Tissue Engineering, S. K. C. xelebier, S. Bozdagˇ Pehlivan, M. Demirbilek, M. Akıncı,* I. Vural, Y. Akdagˇ, S.Yürüker, and N. Ünlü, J. Ocul. Pharmacol. Ther. 2020, Accept

2. 3D printing of biomimetic vasculature for tissue regeneration, Dong Lei, Yang Yang, Z. Liu, B. Yang, W. Gong, S. Chen, S. Wang, L. Sun, B. Song, H. Xuan, X. Mo, B. Sun, S. Li, Q. Yang, S. Huang, S. Chen, Y. Ma, W. Liu, C. He, B. Zhu, E. M. Jeffries, F.-L. Qing, X. Ye,* Q. Zhao* and Z. You, * Mater. Horiz., 6, 2019

3. Mesenchymal stem cell 3D encapsulation technologies for biomimetic microenvironment in tissue regeneration, H. Kim, C. Bae, Y.-M. Kook, W.-G. Koh, K. Lee* and M. H. Park*, Stem Cell Research & Therapy, 10(51), 2019

4. Bioinks and bioprinting technologies to make heterogeneous and biomimetic tissue constructs, N. Ashammakhi, S. Ahadian, C. Xu, H. Montazerian, H. Ko, R. Nasiri, N. Barros, A. Khademhosseini, Material Today Bio, 1, 2019

5. 3D Printing for Tissue Engineering Applications, A. Hacioglu, H. Yilmazer, C. B. Ustundag, Politeknik Dergisi, 21(1), 2018